POD

Proper Orthogonal Decomposition

$$\mathbf{U}(\mathbf{X},t) = \sum_{n=1}^{\infty} \underline{a_n(t)}\ \underline{\mathbf{\Phi}^{(n)}(\mathbf{X})}$$

POD eigenfunctions are representative of flow organisation

POD coefficients are representative of flow dynamics

POD has to be applied to inhomogeneous directions

POD (fundamentals)

Eigenfunctions are obtained by solving an optimisation problem:

Find the *directions* $\mathbf{\Phi}$ as *parallel* as possible to the realisations **u** of the flow ie with an inner product (**u**,$\mathbf{\Phi}$) maximum (average <.>)

The inner product (**u**,$\mathbf{\Phi}$) is the POD projection coefficient $a_n(t)$

$$\left(\ \mathbf{U}(\mathbf{X})\ ,\ \mathbf{\Phi}(\mathbf{X})\ \right) = \int_{\mathcal{D}} \mathbf{U}(\mathbf{X})\ \mathbf{\Phi}(\mathbf{X})\, d\mathbf{X}$$

$$a_n(t) = \left(\ \mathbf{U}(\mathbf{X},t)\ ,\ \mathbf{\Phi}^{(n)}(\mathbf{X})\ \right)$$

Problem to be solved:

Eigenvalue Fredholm integral problem (kernel 2 point correlation tensor)

$$\int_{\mathcal{D}} \underline{\langle\ \mathbf{U}(\mathbf{X})\,\mathbf{U}(\mathbf{X}')\ \rangle}\ \mathbf{\Phi}^{(n)}(\mathbf{X})\, d\mathbf{X} = \lambda_n \mathbf{\Phi}^{(n)}(\mathbf{X}')$$

LUMLEY **SIROVICH**

$$u_i(x,y,z,t) = \sum_{n=1}^{\infty} a_n(t)\Phi_i^{(n)}(x,y,z)$$

Direct POD

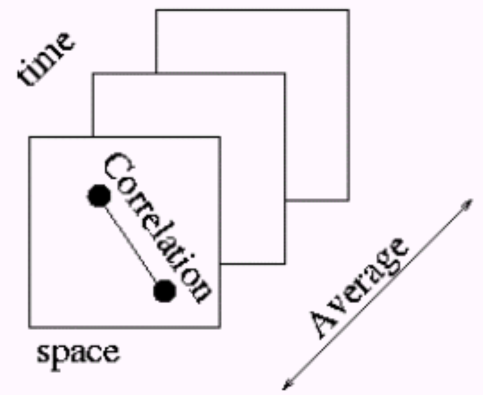

Snapshot POD

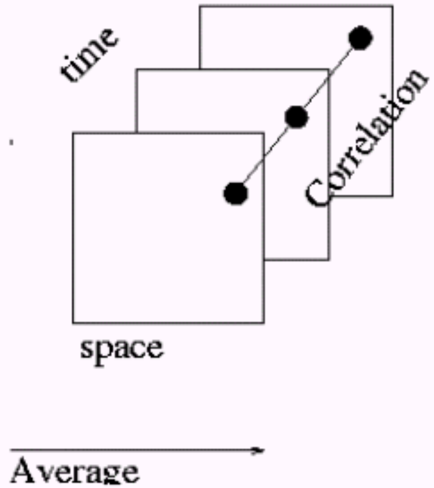

LUMLEY	SIROVICH
few spatial nodes	dense spatial nodes
long time samples	short time samples
Hot/cold wire, microphones	computations, PIV, flow vis.

Direct POD

Considering a formal approach, a 'structure' $\Phi(\underline{X})$ can be defined as the flow realisation with the maximum projection (mean square point of view) on the velocity field $\underline{u}(\underline{X})$. Here Φ is deterministic (ie steady), $\underline{u}$ is random. Therefore one searches for Φ maximizing $\overline{|u.\Phi|^2} = \overline{|\alpha|^2}$ with an inner product (or norm) to be defined following the problem in concern. This concept leads to an eigenvalue type problem:

$$\boxed{\int_D R_{ij}(\underline{X},\underline{X}')\,\Phi_j(\underline{X}')\,d\underline{X}' = \lambda\,\Phi_i(\underline{X})} \tag{2}$$

where R_{ij} is the two point correlation tensor. Following the 'classical' POD, the inner product is defined as:

$$\boxed{(\underline{U},\underline{\Phi}) = \int_D \underline{U}(\underline{X})\underline{\Phi}^*(\underline{X})\,d\underline{X}} \tag{3}$$

For a non-inhomogeneous, periodic or stationnary direction, a harmonic decomposition (Fourier transform) has to be used and the more generic form of the POD problem becomes:

$$\boxed{\int_D \Psi_{ij}(\underline{X},\underline{X}';\underline{k})\Phi_j^{(n)}(\underline{X};\underline{k})\,d\underline{X}' = \lambda^{(n)}(\underline{k}).\Phi_i^{(n)}(\underline{X};\underline{k}),}$$

Snapshot POD

The *Snapshot* POD [Sirovich, 1987] can be illustrated by the *rhs* of the preceding figure. In this case, a spatial average is performed and the kernel of the POD problem is now a time-correlation:

$$\begin{aligned} \boxed{C(t,t') = \frac{1}{T}\int_D u_i(\underline{X},t)u_i(\underline{X},t')\,d\underline{X}} \\ = \frac{1}{T}\sum_{n=1}^{N_{POD}} a^{(n)}(t)a^{(n)}(t'). \end{aligned} \tag{10}$$

The eigenvalue problem to solve is then:

$$\boxed{\int_T C(t,t')a^{(n)}(t')dt' = \lambda^{(n)}a^{(n)}(t),} \tag{11}$$

the 'spatial' eigenfunctions are afterward obtained by projection

$$\Phi^{(n)}(\underline{X}) = \frac{1}{T}\frac{1}{\lambda^{(n)}}\int_T u_i(\underline{X},t)a^{(n)}(t)dt \tag{12}$$

Direct POD

- Moin & Moser (J.F.M 1989) DNS of a Channel Flow

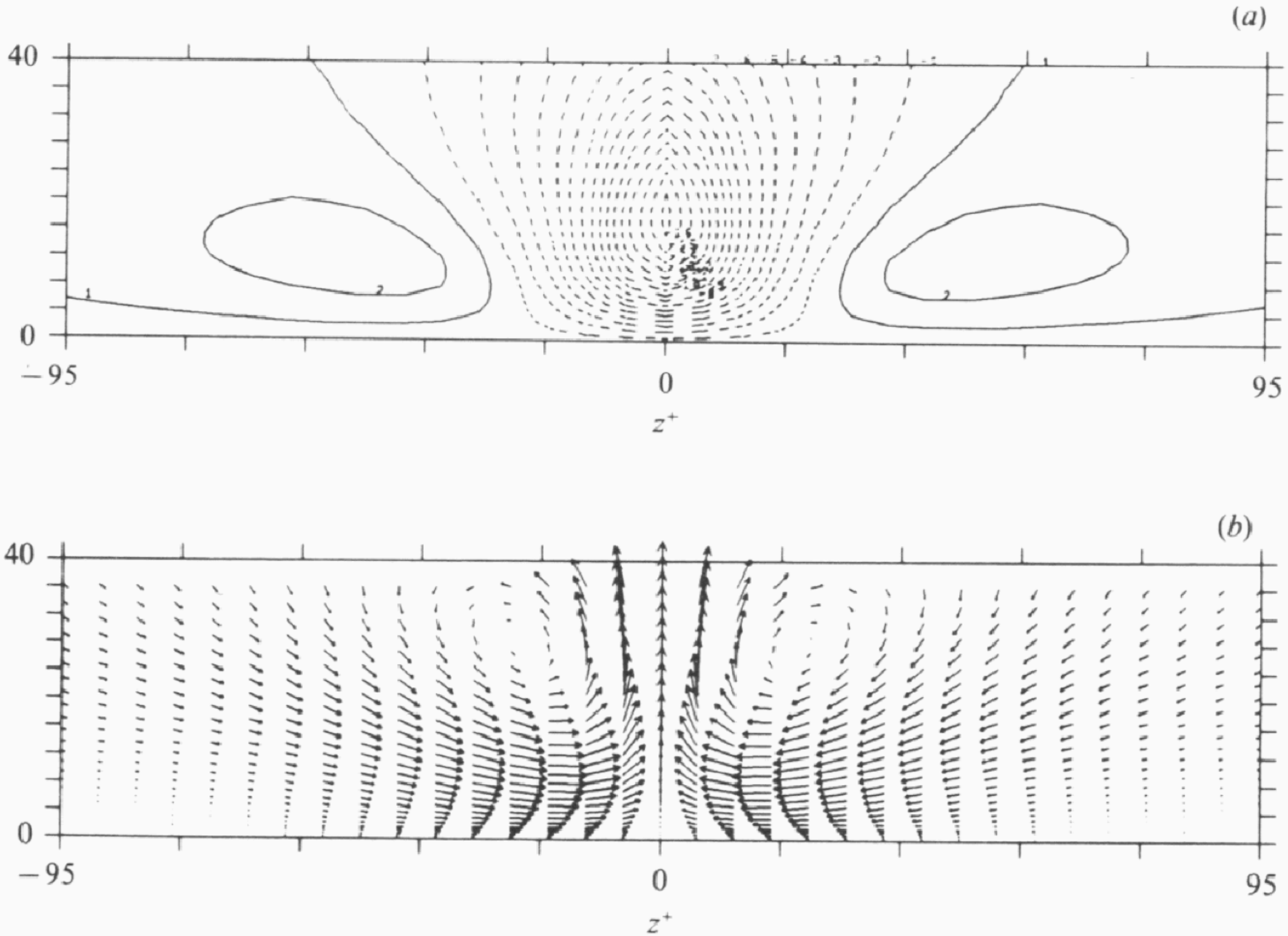

FIGURE 10. Two-dimensional zero-phase characteristic eddy in the near-wall domain ($y^+ \leqslant 40$), (a) contours of u and (b) velocity vectors projected into the (y, z)-plane. Contour increment in (a) is 1. Negative contours are dashed.

Snapshot POD

- Sirovich & Kirby (J. of Opt. Soc. 1987)

Fig. 1. Average face based on an ensemble of 115 faces. In this, as in the other plates, we have refrained from filtering out the high frequencies produced by the digitization. A pleasanter picture can be had by the usual trick of squinting or otherwise blurring the picture.

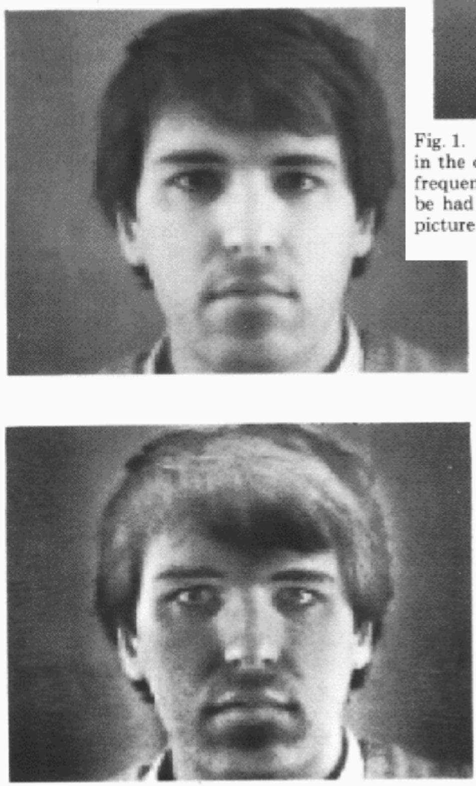

Fig. 2. Sample face on top and its caricature below it.

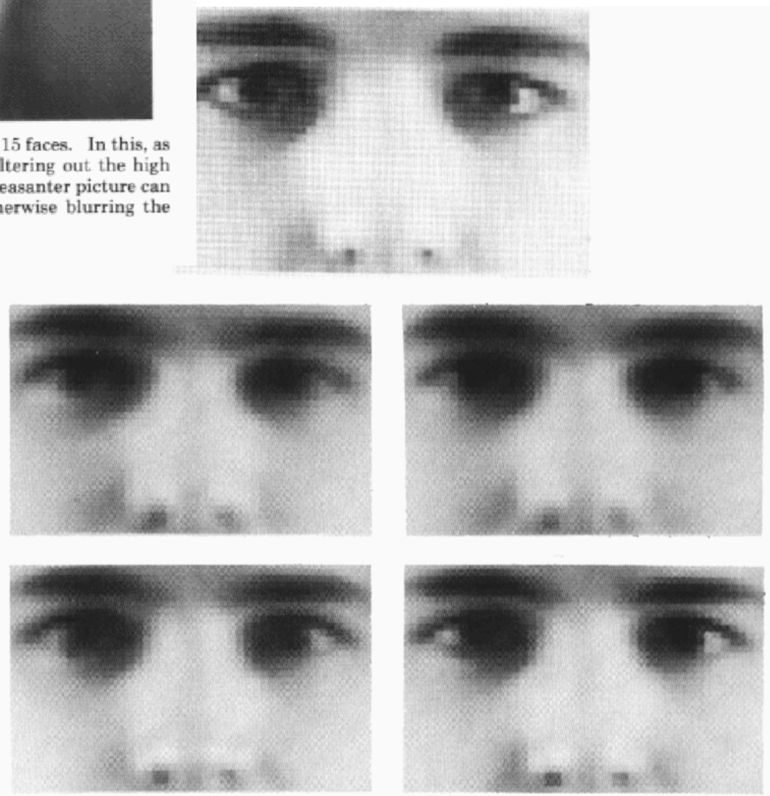

P Fig. 5. Approximation to the exact picture (middle panel of Fig. 3) using 10, 20, 30, and 40 eigenpictures.

LODS Identification
(calibration, assimilation,…)

Development of Low Order Dynamical Systems (LODS) from *reduced* sets arising from experimental/numerical data bases

Time or non-time resolved information, however representative of the flow dynamics

- ✓ Total or partial Velocity field
- ✓ Scalar quantity (concentration, pressure)

\+ POD based Identification technique

Practical Generation of Video Textures using the Auto-Regressive Process

Neill Campbell, Colin Dalton, David Gibson and Barry Thomas
Department of Computer Science
University of Bristol
Bristol, BS8 1UB
Neill.Campbell@bristol.ac.uk

The "Campfire"

Starting from the

video of a campfire

POD analysis

AR modeling the **a's**

Virtual campfire

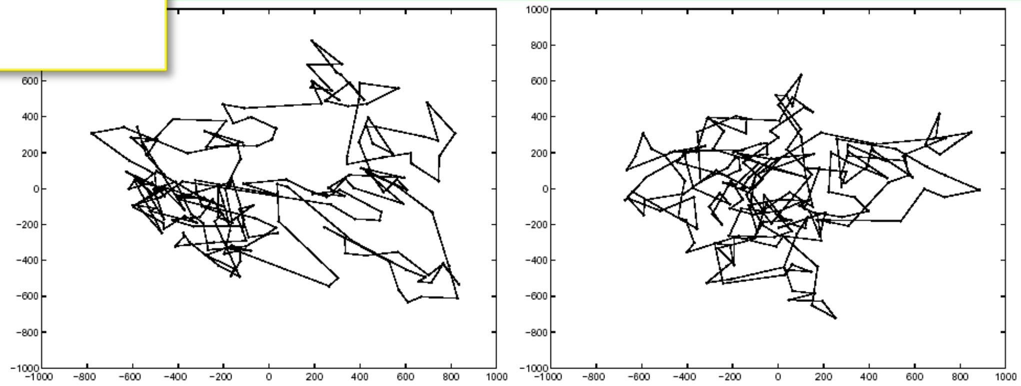

Figure 1: (Left) The original campfire sequence projected into a two-dimensional eigenspace for clarity. It is this 'signature' that we aim to model automatically. The axes show response to the dominant eigenvectors of the campfire images. (Right) One reconstruction of the campfire signature automatically generated using an auto-regressive model.

Figure 2: Three of the resulting frames from the new sequence of the campfire. All frames are synthesised, never having appeared in the original clip.

LODS Identification

Aims: subset of the Dynamical System

- *POD-Galerkin like* equations for a scalar quantity or partial information (eg : 2D3C slice of a 3D configuration ...)

$$\frac{da_i}{dt} = M_i + \sum_{j=1}^{N} L_{ij} a_j + \sum_{j=1}^{N} \sum_{k=j}^{N} Q_{ijk} a_j a_k$$

- Identification of the coefficients *M, L, Q* from non-time resolved samples of the 'as' and of their time derivative. Or from time resolved.
  - By using correlations *<da/dt a>* [Verdet 1998, Ricaud 2002]
  - By a *least mean square* approach using ***Singular Value Decomposition*** [Perret et al 2006]

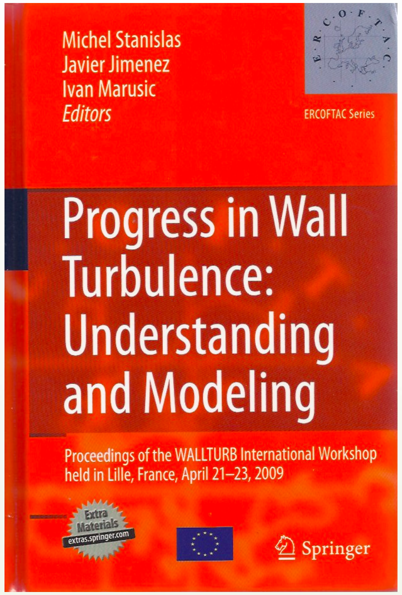

http://calins.limsi.fr

L+ 300

http://wallturb.univ-lille1.fr

A 'model' @ y+=10

CALINS

Dual time stereoscopic PIV

R_θ	7800
Ue [m/s]	3
Temperature [^{o} c]	19
U_τ [m/s]	0.121
Δ_t [μs]	200
y [wall units]	10

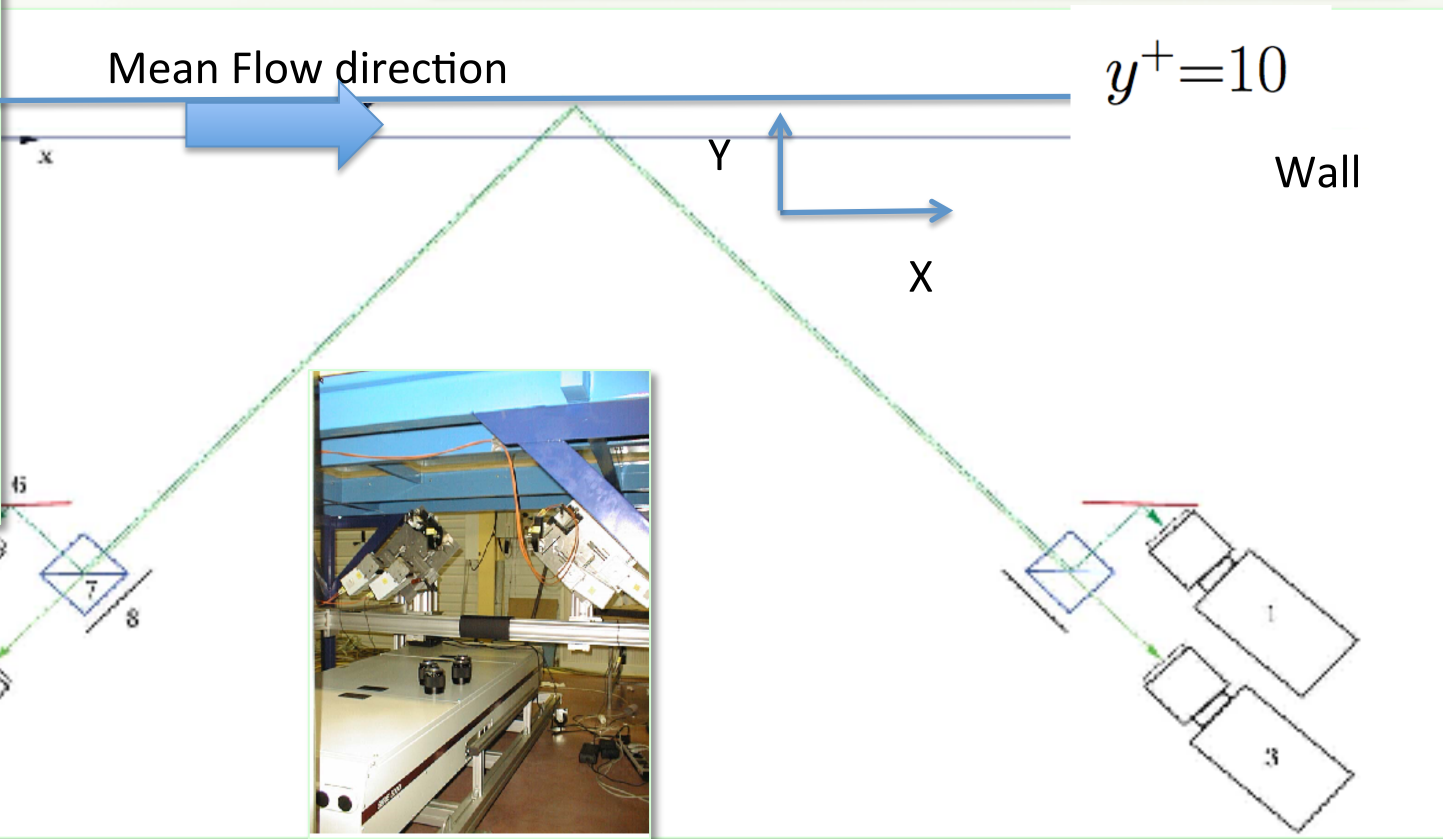

$y^+ = 10 \qquad R_\theta = 7800$

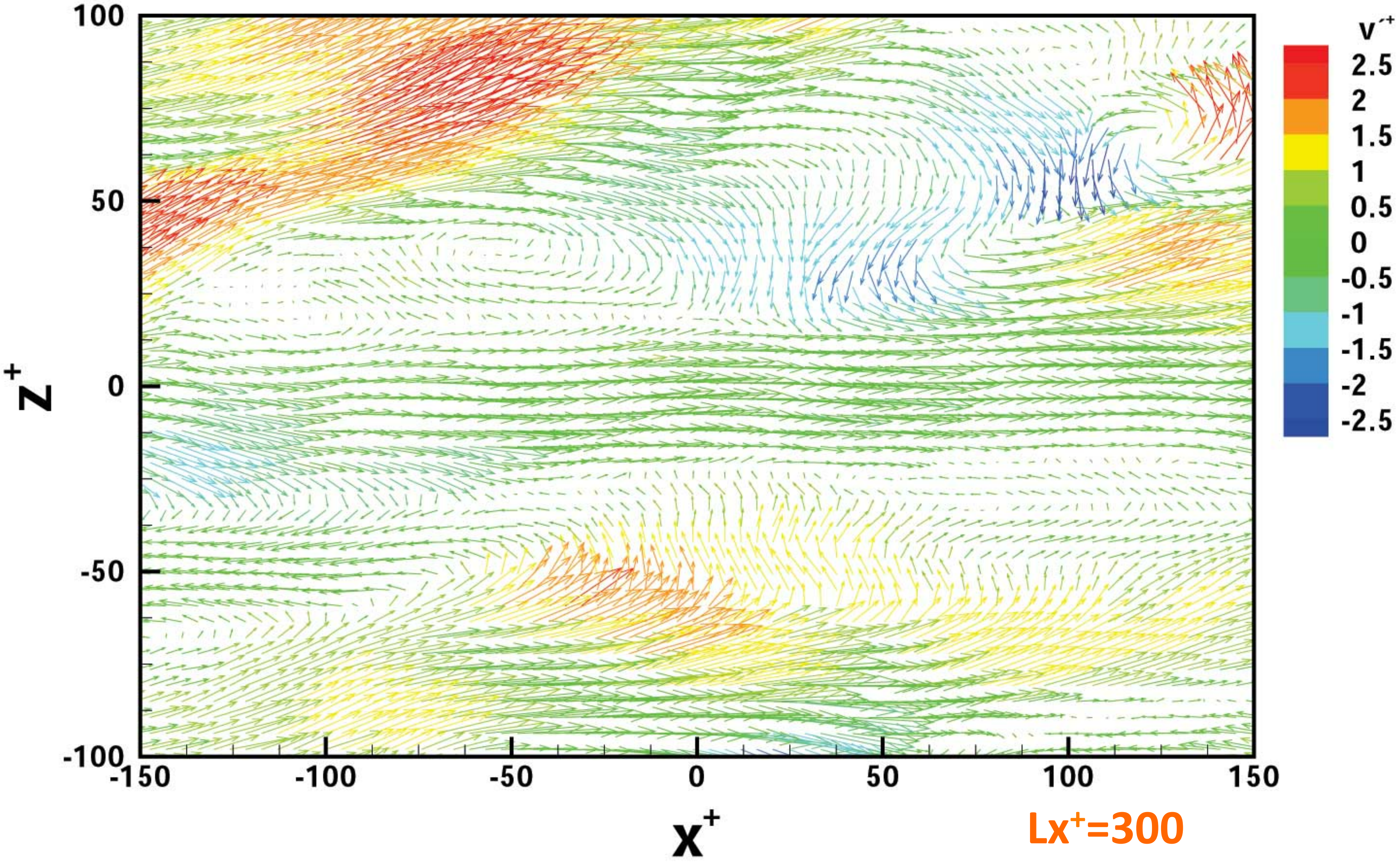

Vectorial POD : POD_{uvw}

$$\int_{\mathcal{D}} R_{ij}(\mathbf{x},\mathbf{x}')\ \Phi_j^{(n)}(\mathbf{x}')d\mathbf{x}' = \lambda_n\ \Phi_i^{(n)}(\mathbf{x})$$

Scalar POD : POD_u

$$\int_{\mathcal{D}} R_{ii}(\mathbf{x},\mathbf{x}')\Phi_i(\mathbf{x}')\ d\mathbf{x}' = \lambda\Phi_i(\mathbf{x})$$

POD analysis of DB1

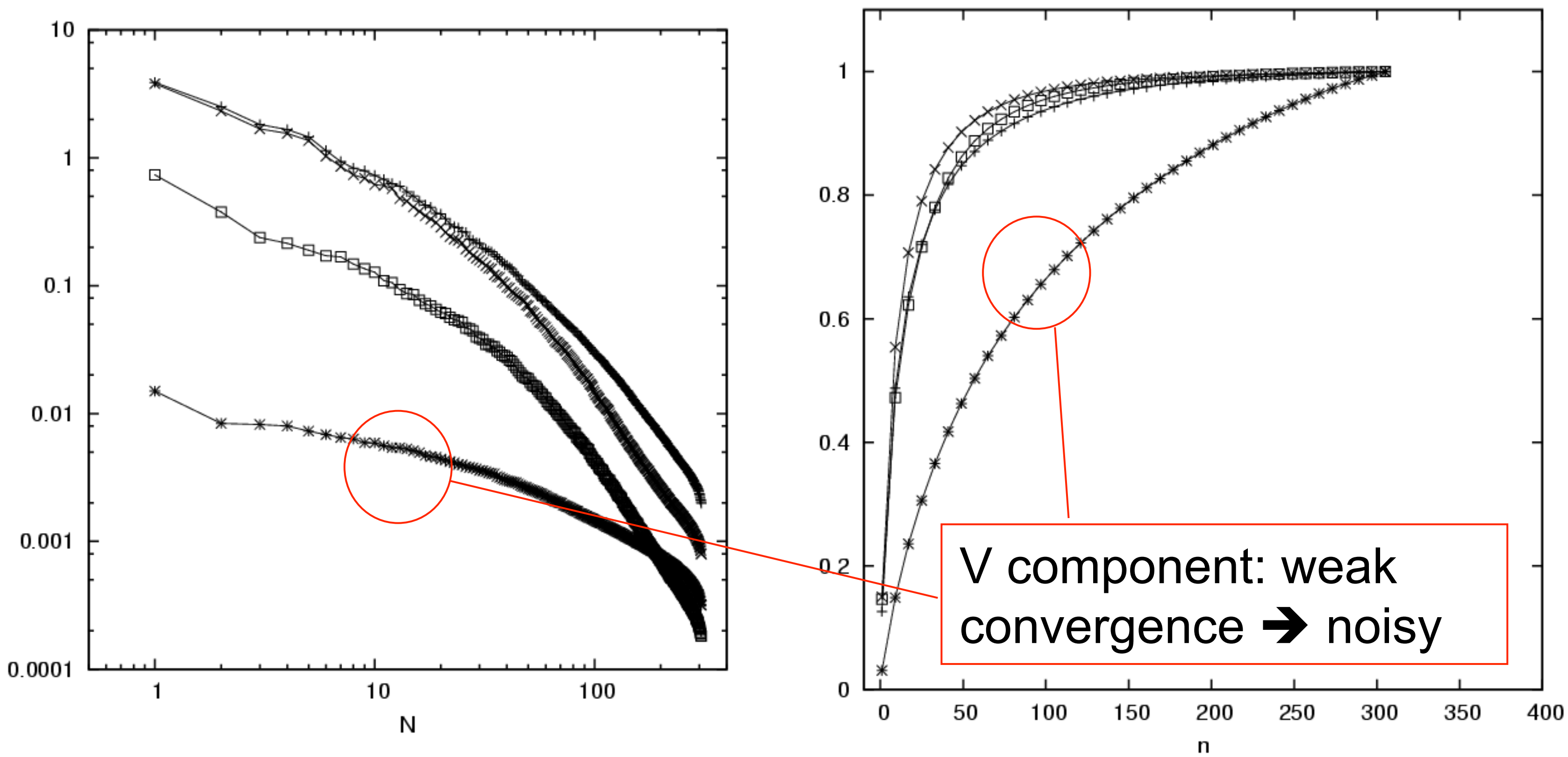

Figure 19: Eigenvalue spectrum (left) and convergence of POD modes (right). $+$ POD_{uvw}, $\times$ POD_u, $\square$ POD_w and $\star$ POD_v

CALINS

$y^{+}=10$ $\quad R_\theta = 7800$

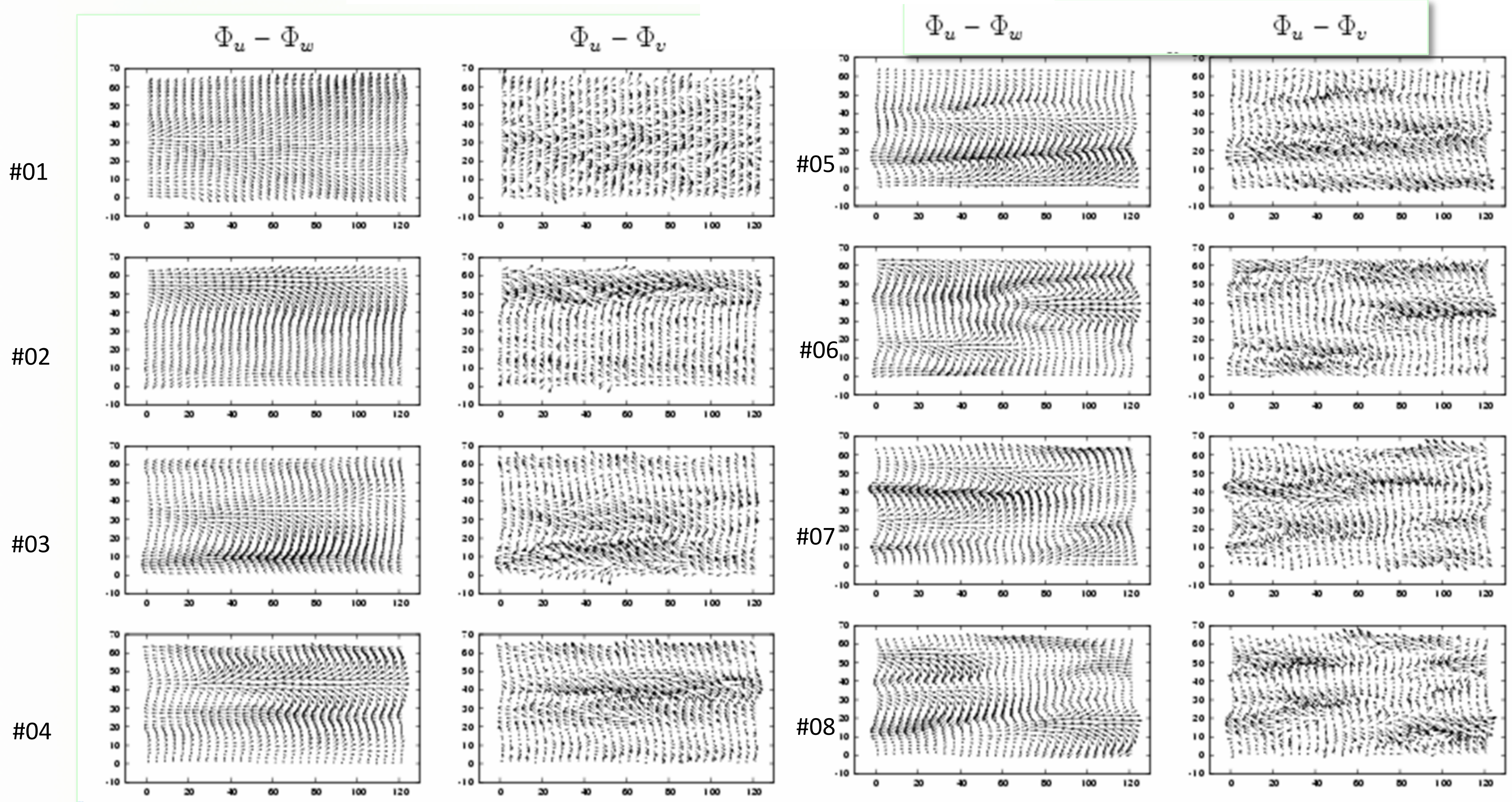

Figure 21: Velocity fields of the first eight POD modes of the boundary layer (top to bottom). The plots are seen in a xz–plane: uw components in the xz–plane (left) ; uv in the xz–plane (left).

In a 2T SPIV approach it is required that the POD modes remains *coherent* between times t (PIV1) and t+τ (PIV2)

$$\alpha_n = \int_{\mathcal{D}} \Phi^{(n)}_{\mathrm{piv1}}(x)\Phi^{(n)}_{\mathrm{piv2}}(x)\ dx$$

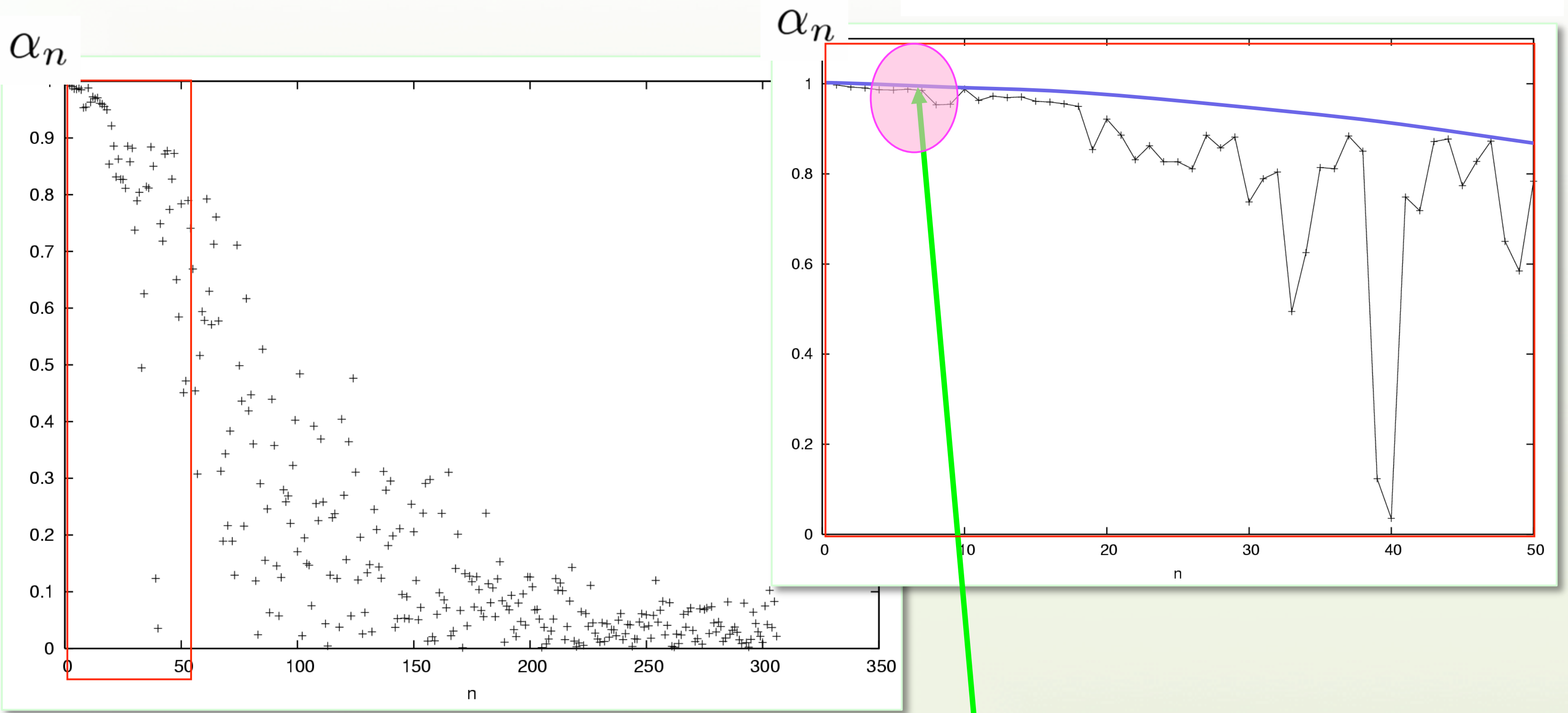

➔We can expect a decrease of α_n due to stastical considerations

➔Discrepancies from this decay are linked to PIV ‘noise measurement’

➔We can then define the maximum number of POD modes that can be considered at most to define a ROM from the experiment

$y^+=10$ $R_\theta = 7800$

We consider here a 4 equation ROM

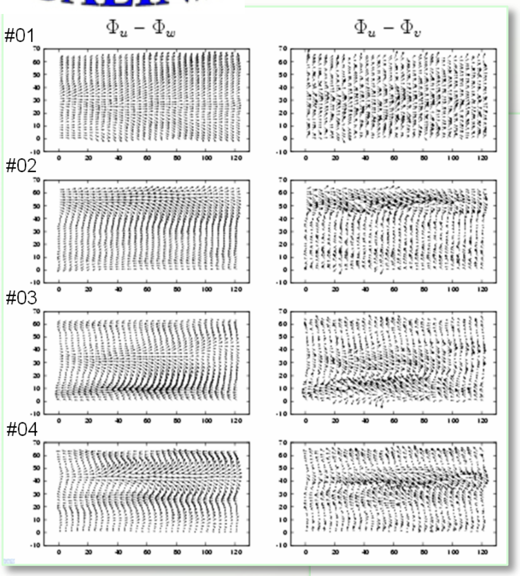

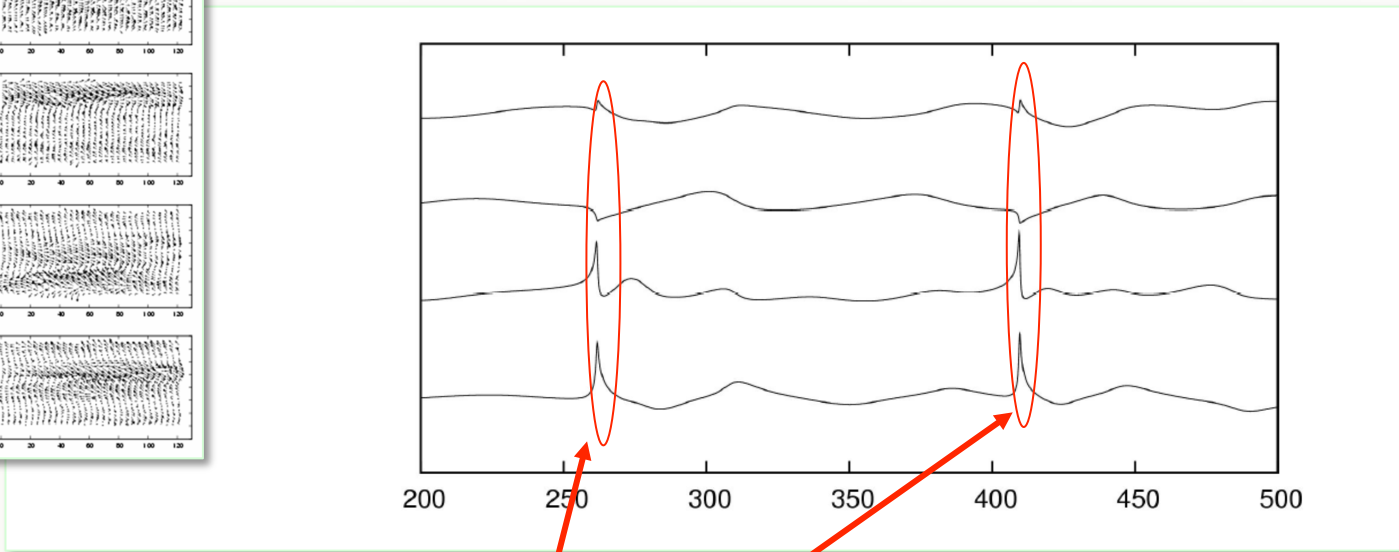

Some intermittent events appear

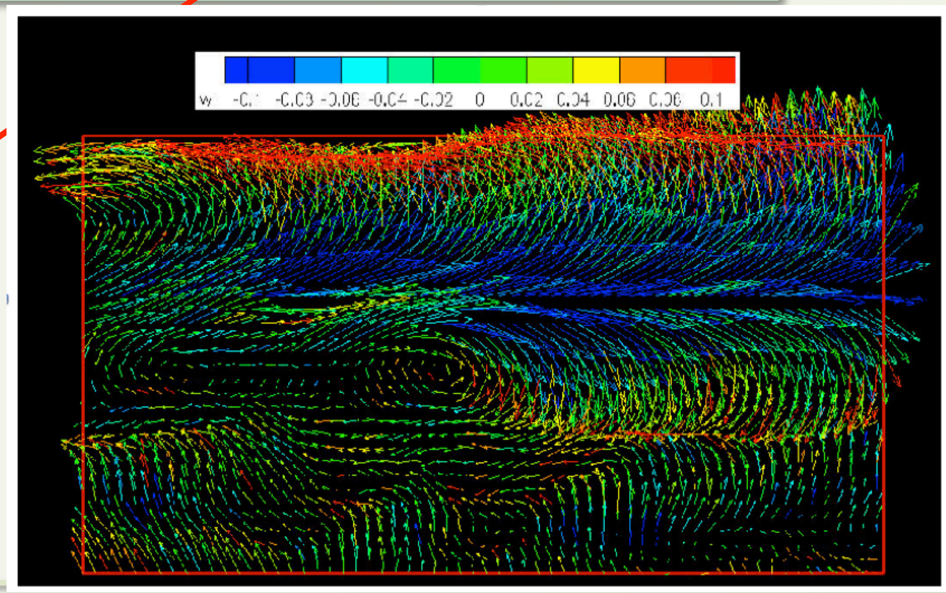

A ‘model’ @ y+=100

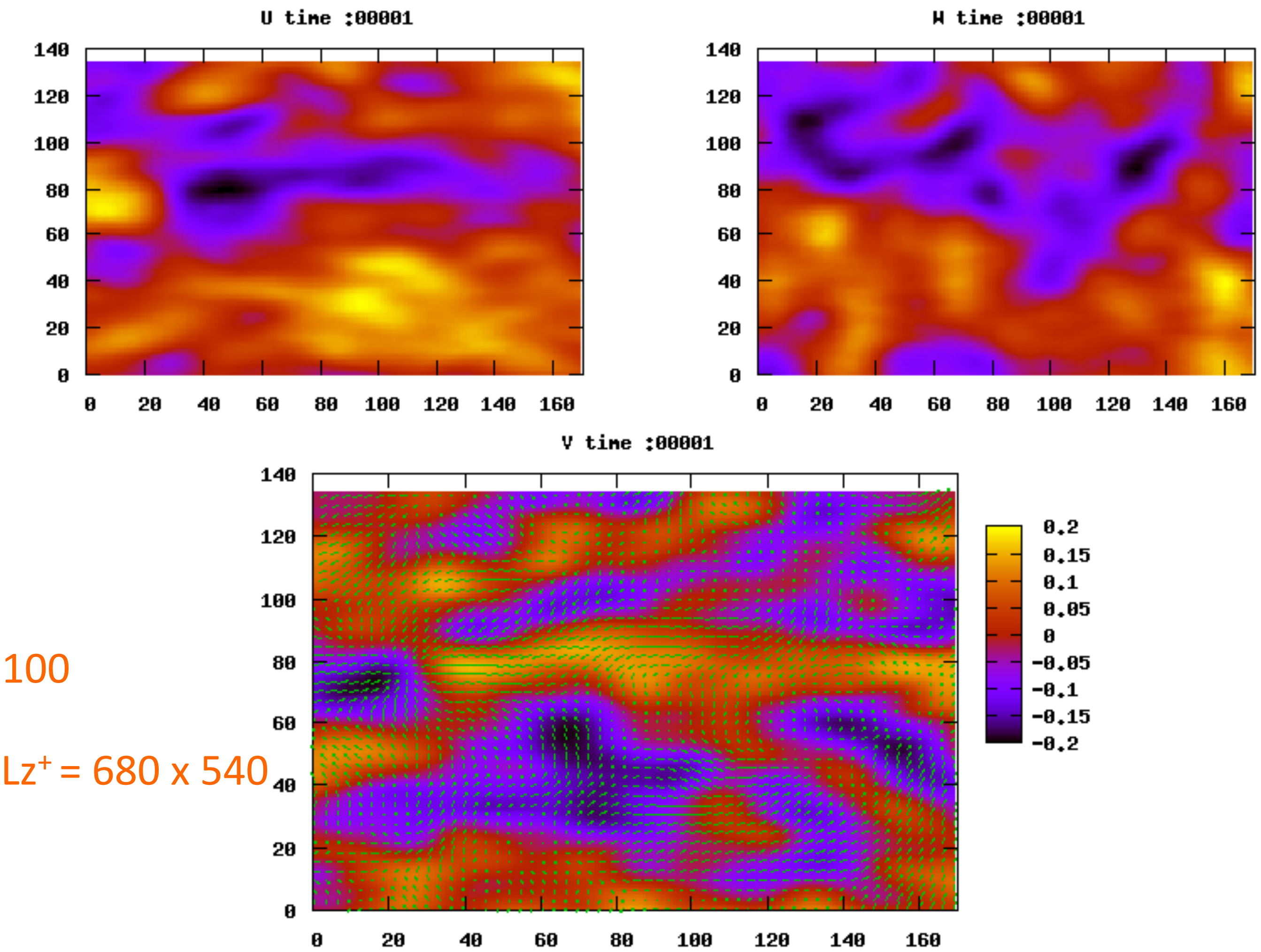

$y^+ = 100$

$Lx^+ \times Lz^+ = 680 \times 540$

- Analysis of POD modes and of their temporal evolution

→ towards Stochastic model for highest modes …

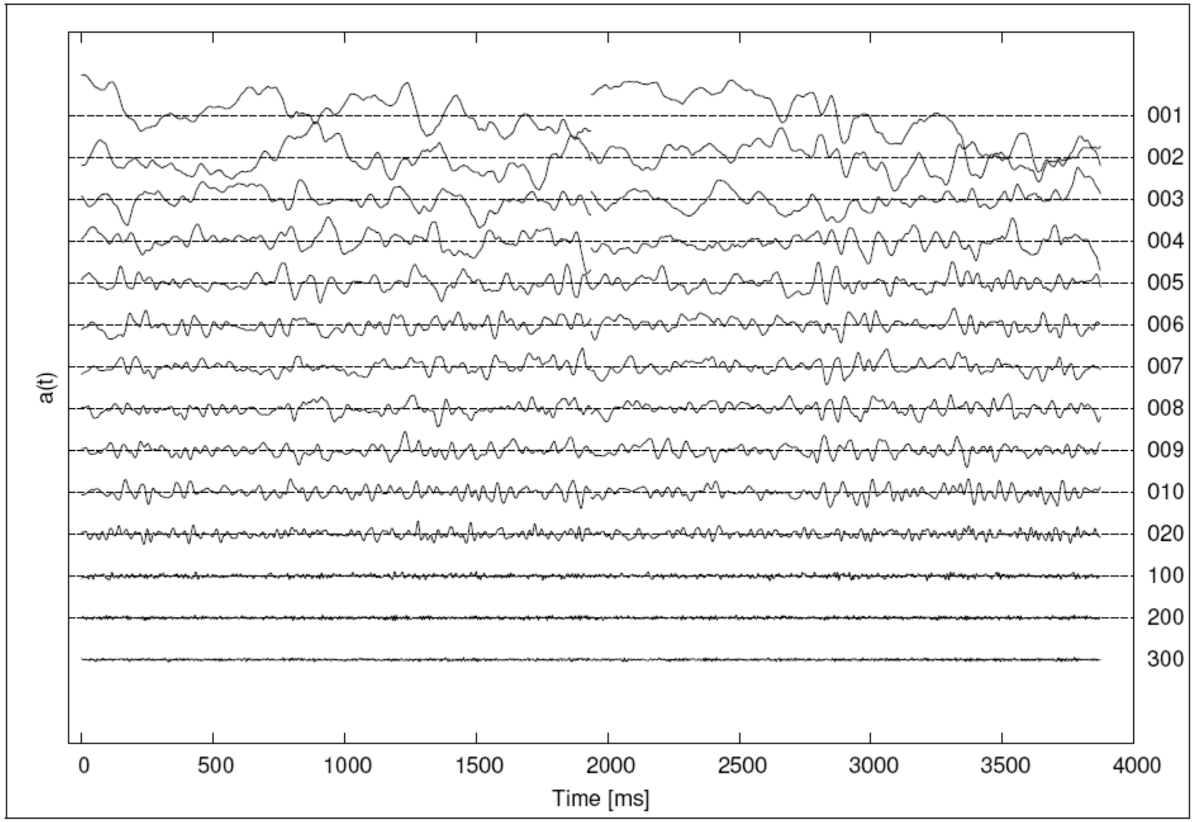

FIG. 8 – Time history of POD projection coefficients $a_n(t)$ for modes 1, 2, $\cdots$, 10 ; 20, 100, 200 and 300.(case **Clong**)

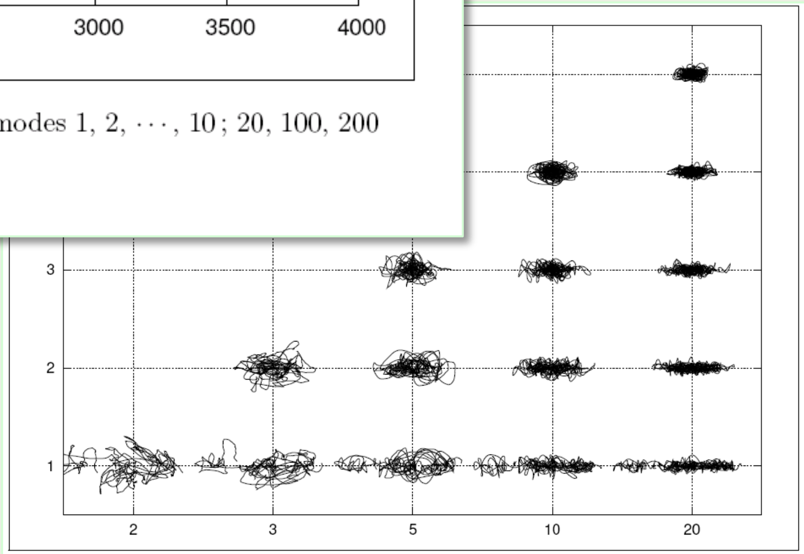

FIG. 9 – Typical phase portraits of selected modes. (case **Clong**)

Time history of $a_n(t)$

$$\lambda_n = < a_n^2 >$$

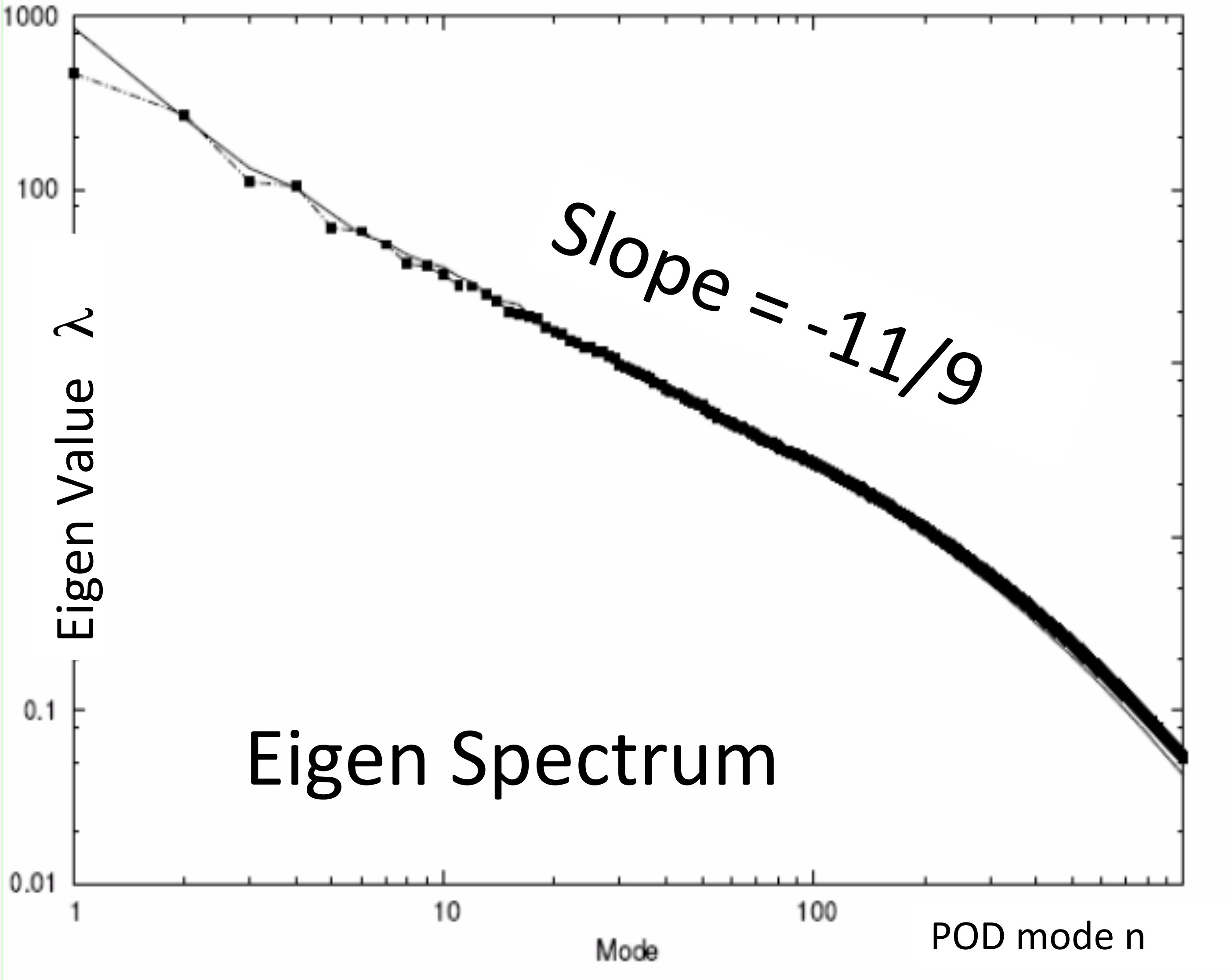

1000
100
0.1
0.01
1
10
100
Mode
Eigen Value λ
Slope = -11/9
Eigen Spectrum
POD mode n

Spectra of $a_n(t)$ $E_n(f) = < \widehat{{}^f a_n(t)} \, \widehat{{}^f a_n(t)}^* >$

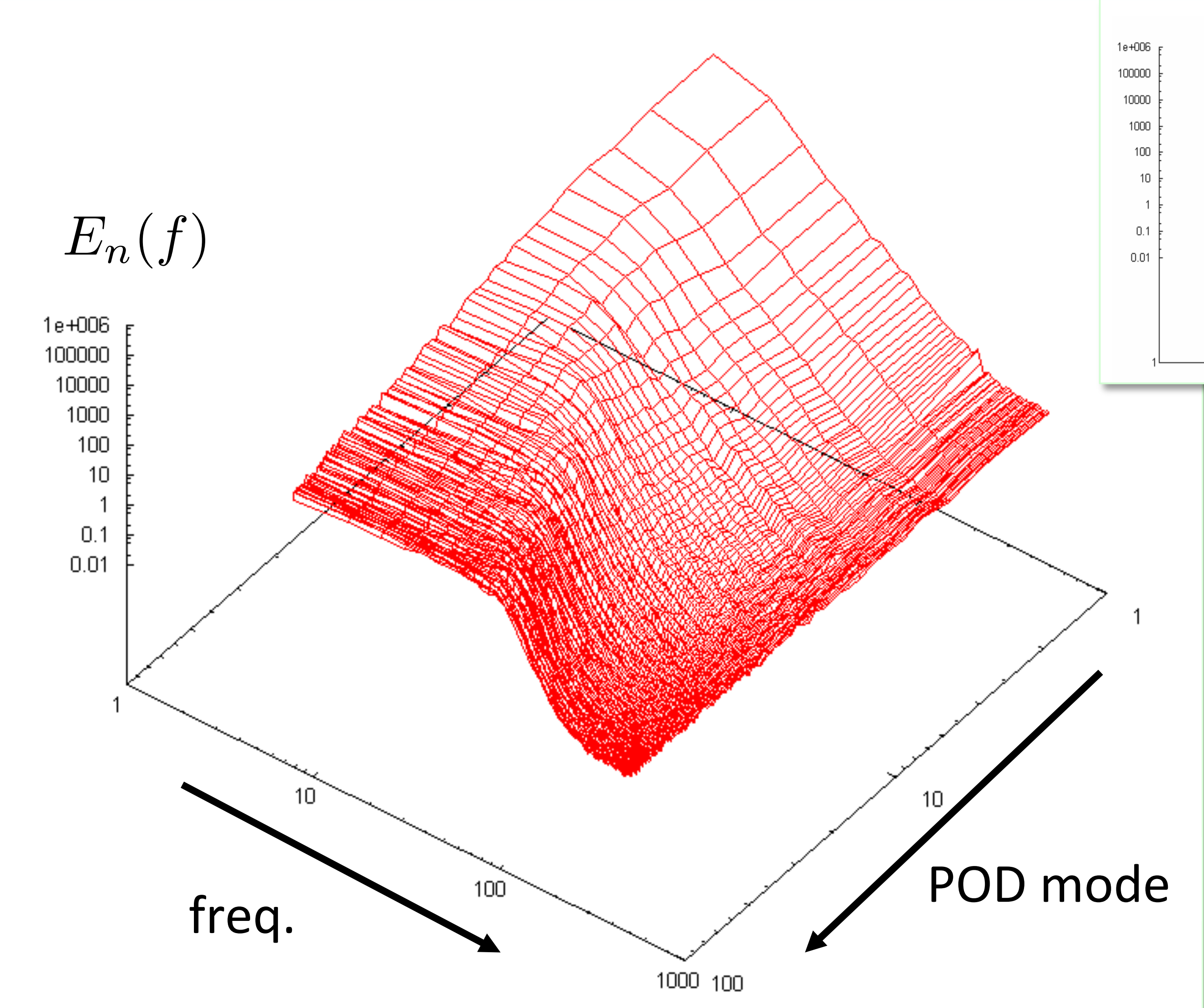

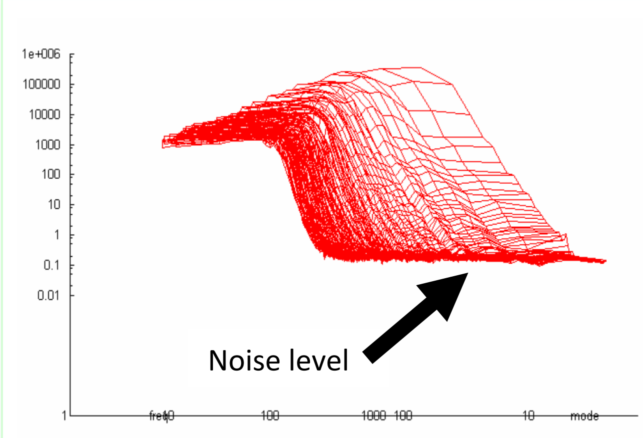

Towards a scaling law

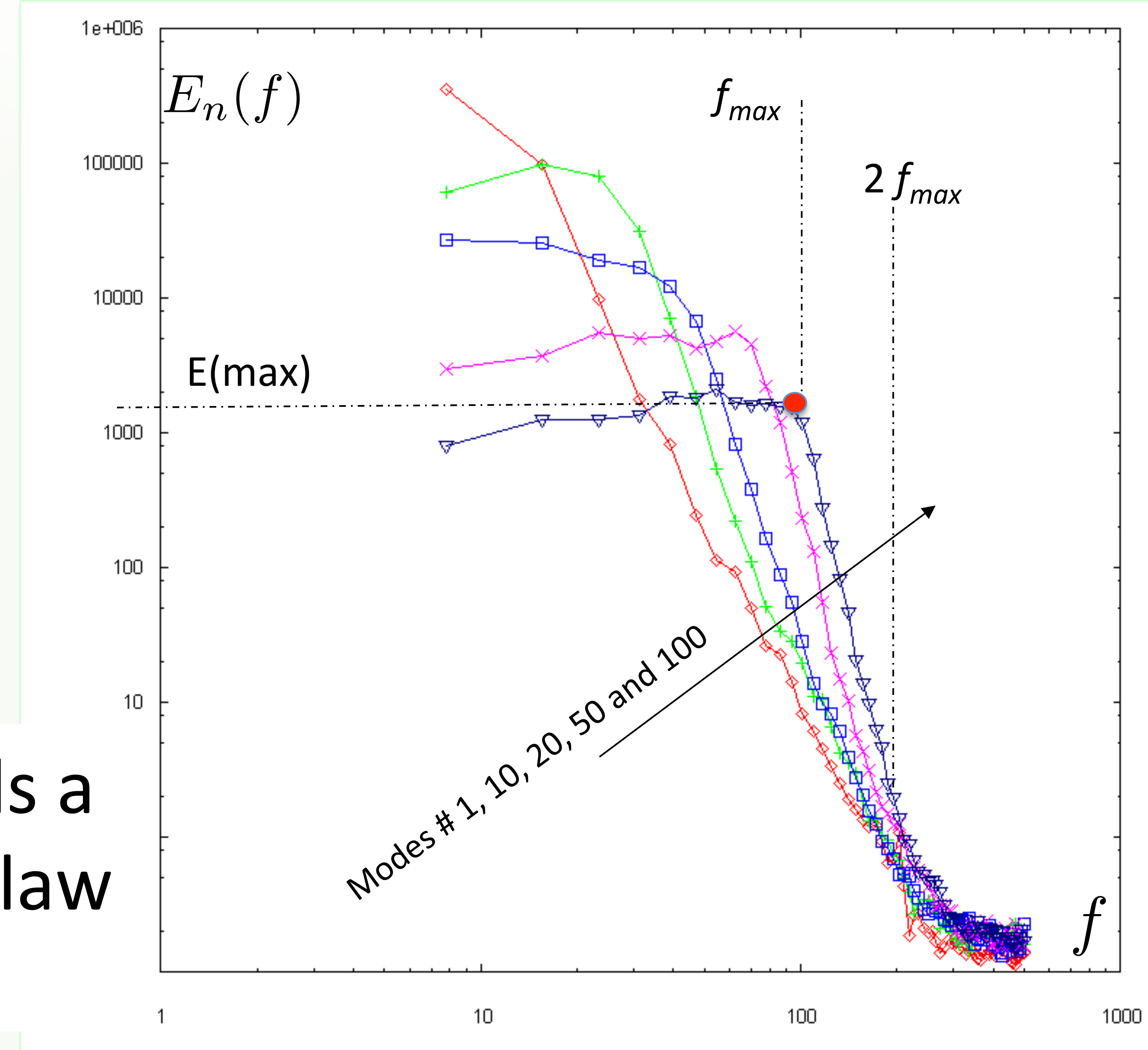

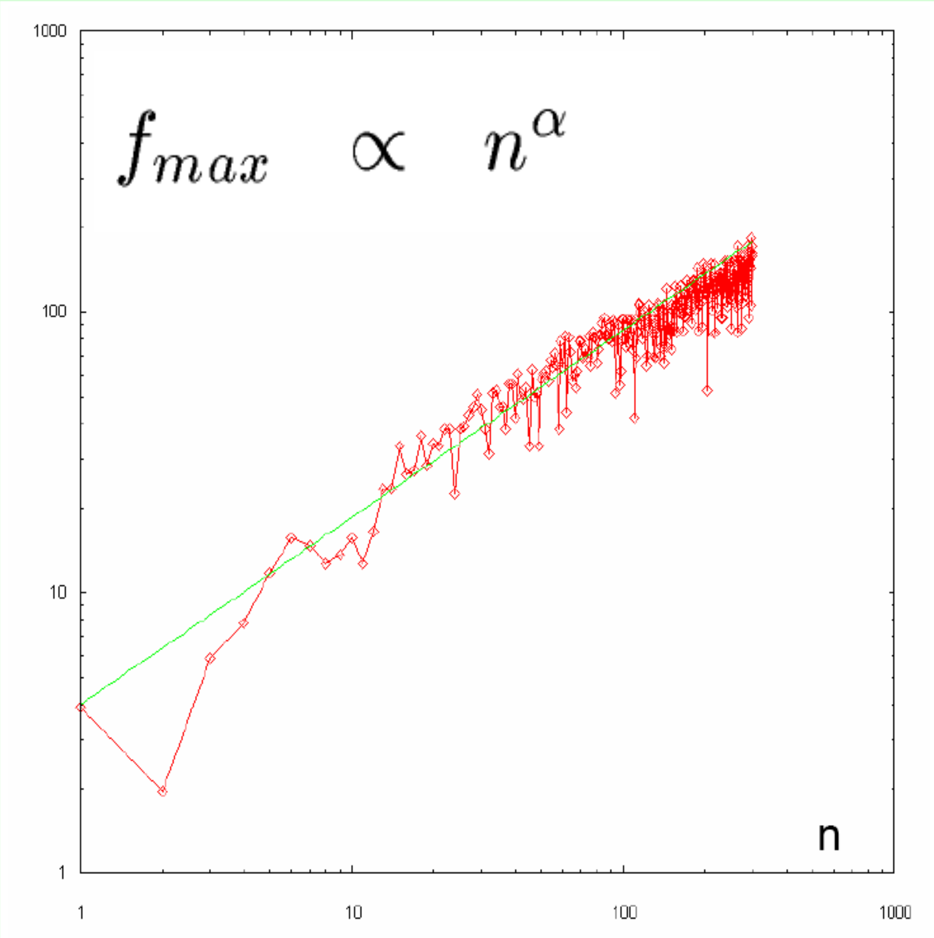

1000
100
10
1
1
10
100
1000
$f_{max} \propto n^{\alpha}$
n

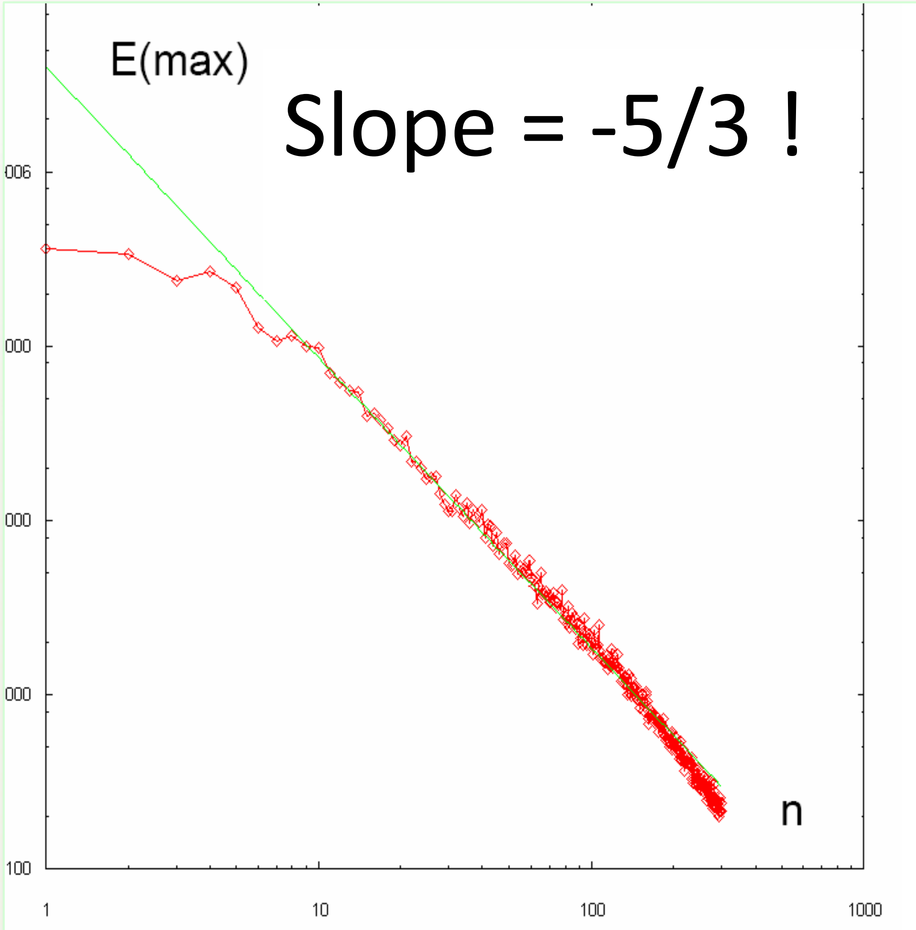

E(max)
Slope = -5/3 !
n
1
10
100
1000

$$\int \lambda_n(f)\,df \;\propto\; n^{-11/9}$$

$$\lambda_n(f) \;\propto\; n^{-5/3} f^{\alpha} \qquad \alpha \simeq 0.5$$

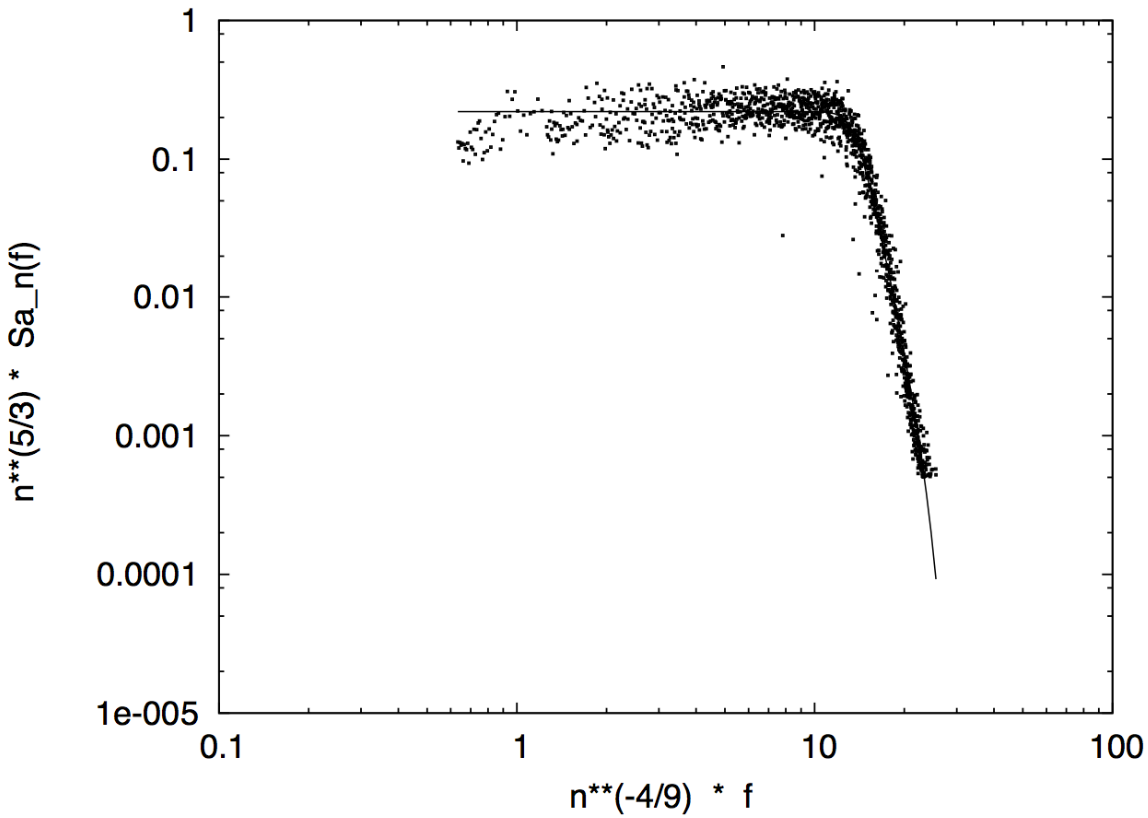

➔ A way for predicting energy distribution of the POD coefficients

$$a_n(t) \simeq \mathrm{IFT}(a_n(f)\exp(j\Phi_{rand}))$$

Correct but phase is missing

➔ i.e No advection, …

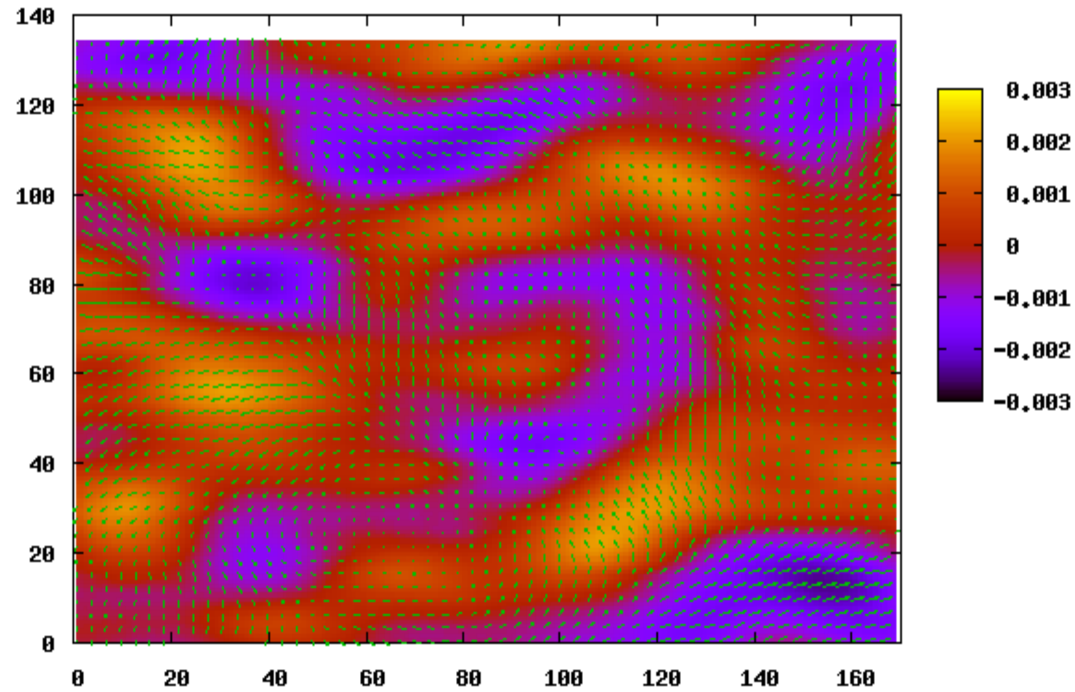

➔ Need to add interactions between modes

Frequency range of linear interactions between POD modes
For given n if it exists (m,f) such that $\gamma_{mn}(f)>0.2$ →

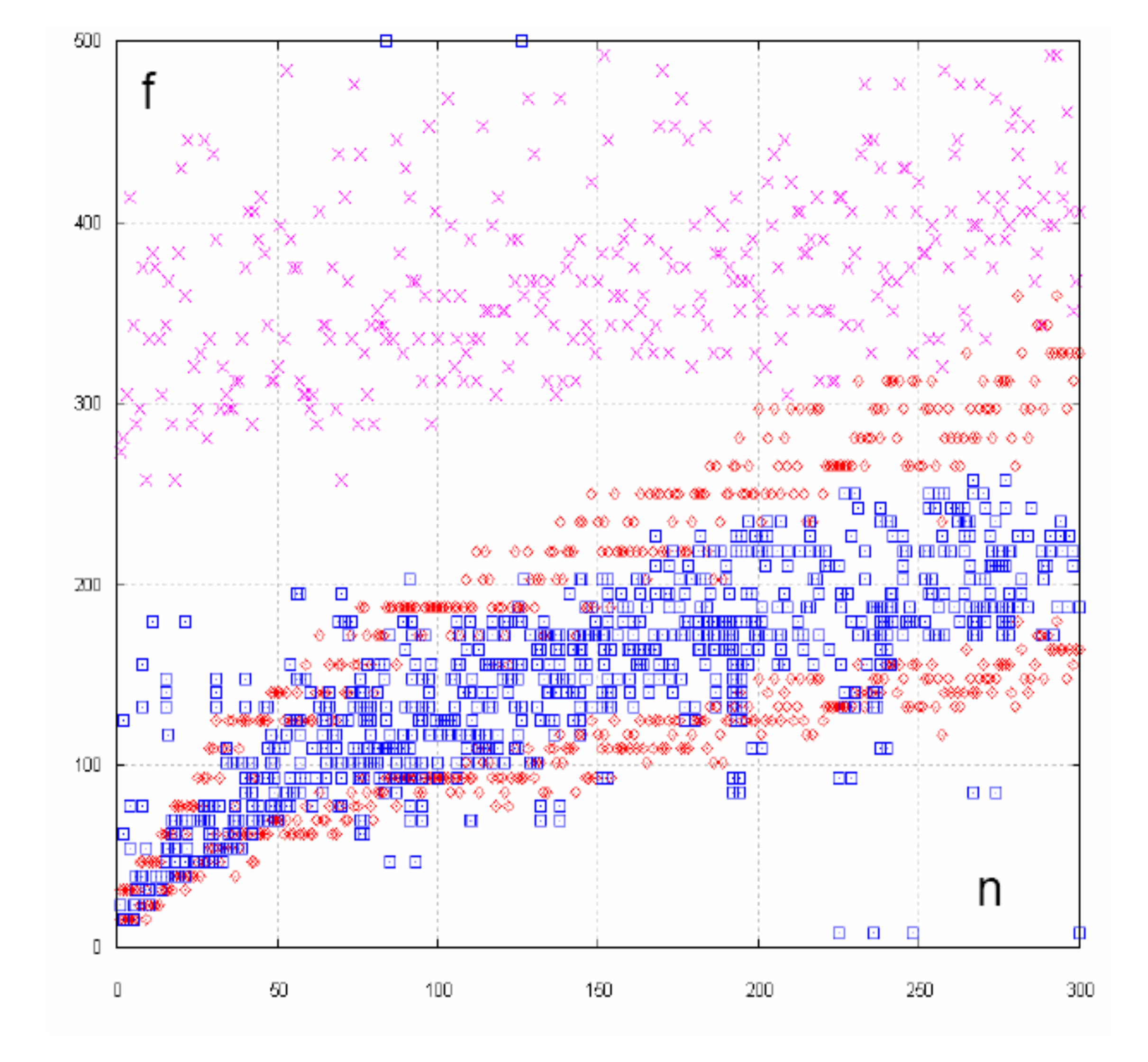

noise

2 x fmax

Modes interaction region

fmax

Same plot taking into account scaling law

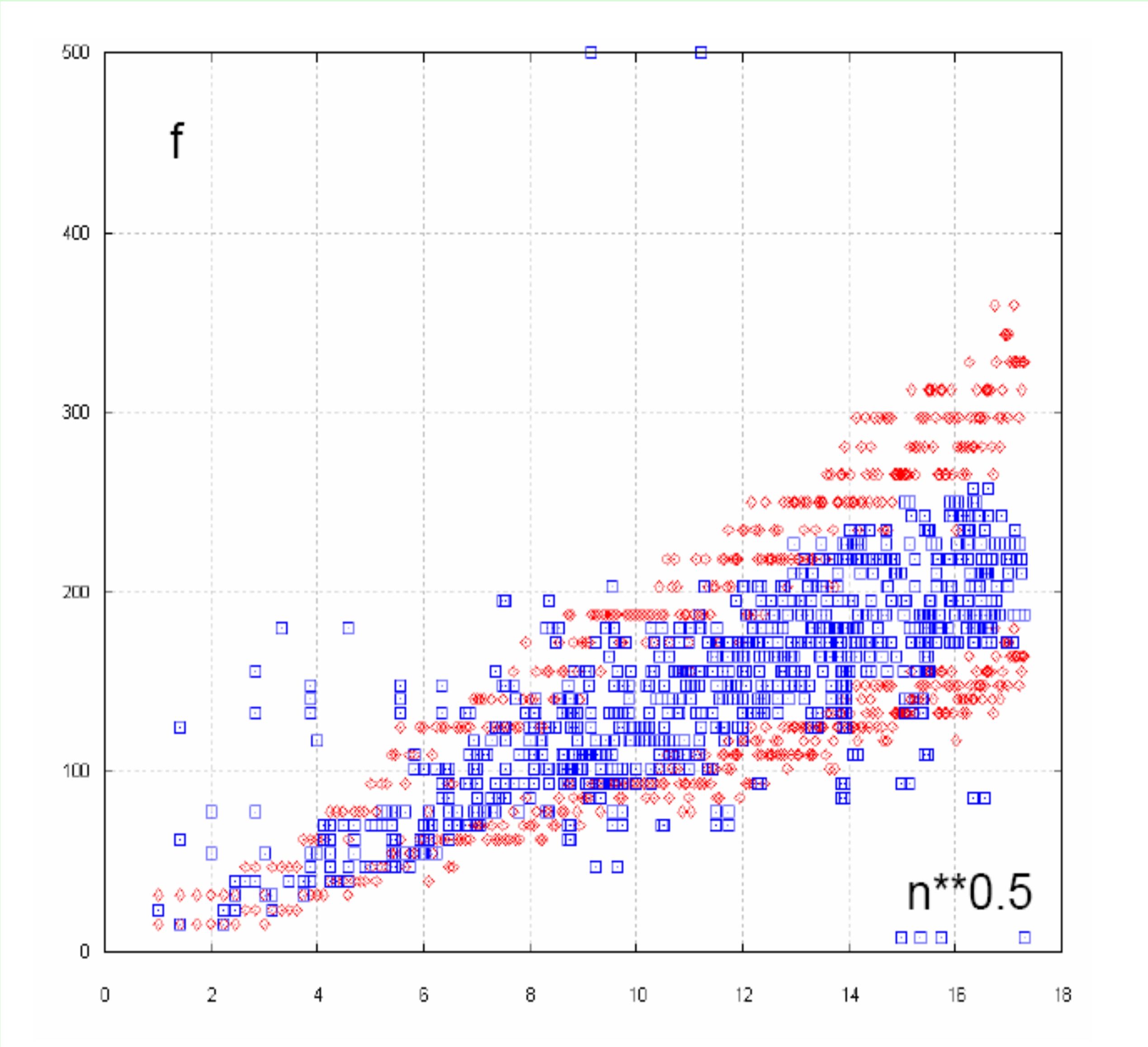

Advection

The main feature of the data under analysis is that an advection exists in the streamwise direction x with a mean convective velocity V. Let us consider a model where only this advection is taken into account.

$$\frac{\partial}{\partial t} u_i(x,z) \ + \ V \ \frac{\partial}{\partial x} u_i(x,z) = 0$$

Introducing the POD decomposition, considering a truncation to N_{tr} modes and if we suppose that the convective velocity is mode independant, this equation writes :

$$\frac{\partial}{\partial t} \sum_{n=1}^{N_{tr}} a_n(t) \Phi_i^{(n)}(x,z) \ + \ V \frac{\partial}{\partial x} \sum_{m=1}^{N_{tr}} a_m(t) \Phi_i^{(m)}(x,z) = 0$$

$$\boxed{< \mathbf{a}_n \ \dot{\mathbf{a}}_p >= -V \ \lambda^{(n)} \ \left(\mathbf{\Phi}_{,x}^{(n)} \ , \ \mathbf{\Phi}^{(p)} \right)}$$

$$A(n,m) = -V \ P(n,m)$$

– the correlation $A(n,m) =< \mathbf{a_n} \ \dot{\mathbf{a}}_m >$ and

– the weighted inner product $P(n,m) = \lambda^{(n)} \ (\mathbf{\Phi}_{,x}^{(n)} \ , \ \mathbf{\Phi}^{(m)})$

are correlated.

$| < a_n \dot{a}_m > |/\lambda^{(n)}$; (b) $|(\Phi_{i,x}^{(n)} \,,\, \Phi_i^{(m)})|$

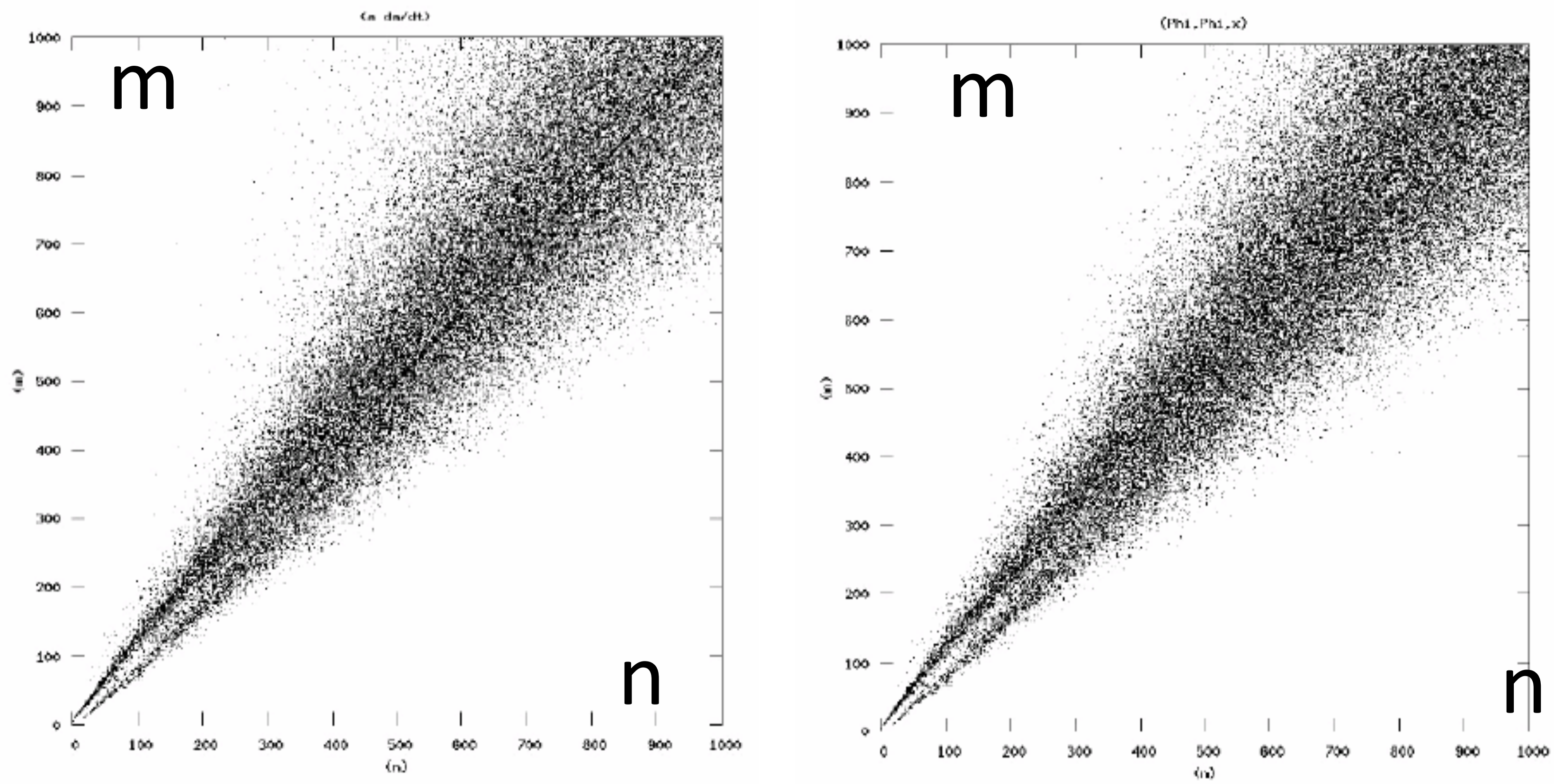

(a)

FIG. 10 – Comparison of : (a) $| < a_n \dot{a}_m > |/\lambda^{(n)}$; (b) $|(\Phi_{i,x}^{(n)} \,,\, \Phi_i^{(m)})|$. Plotted are locations where the local value of these quantities is greater than 17% of their maximum value. (case **Cshort**)

$$| < a_n \dot{a}_m > |/\lambda^{(n)} \text{ ; (b) } |(\Phi_{i,x}^{(n)} \;,\; \Phi_i^{(m)})|$$

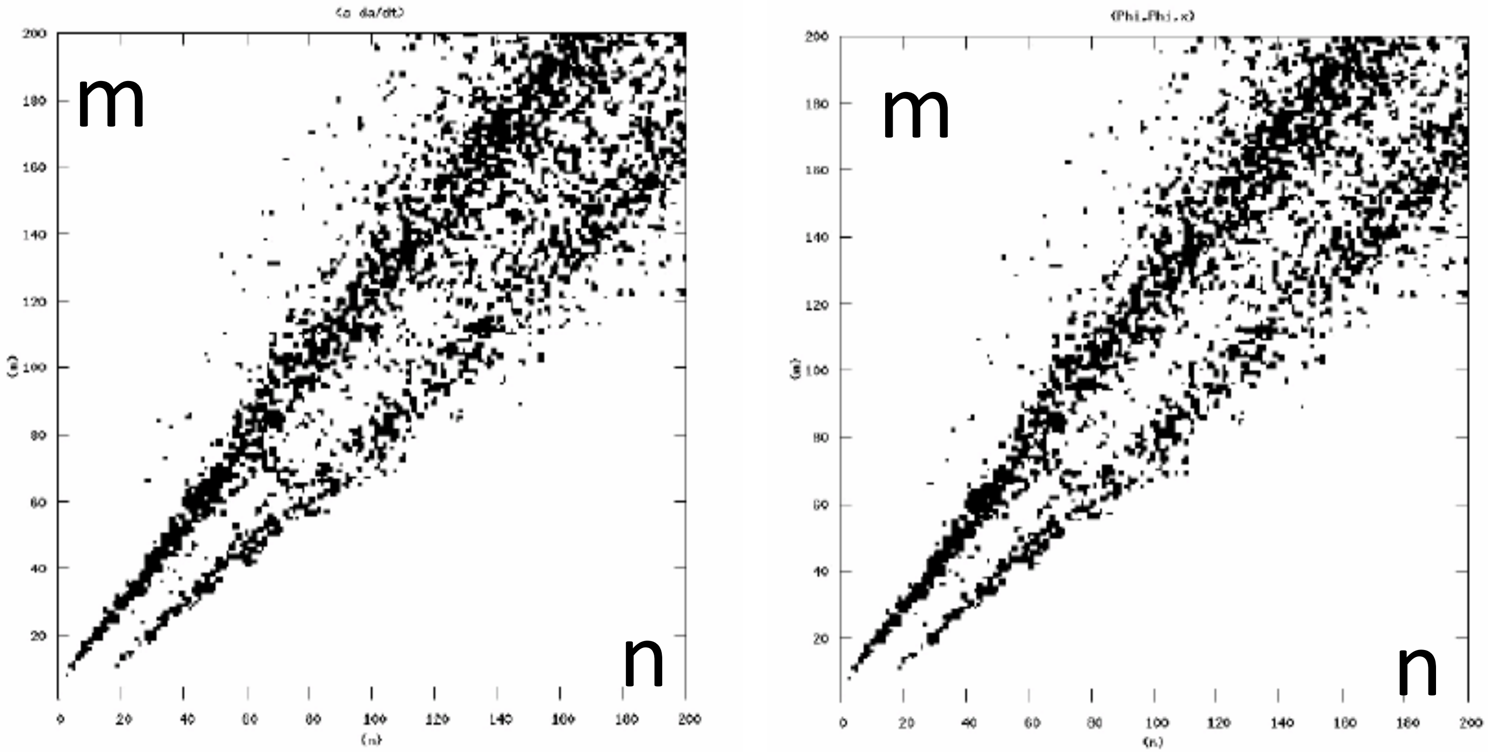

Zoom n<100

Same plot taking into account scaling law

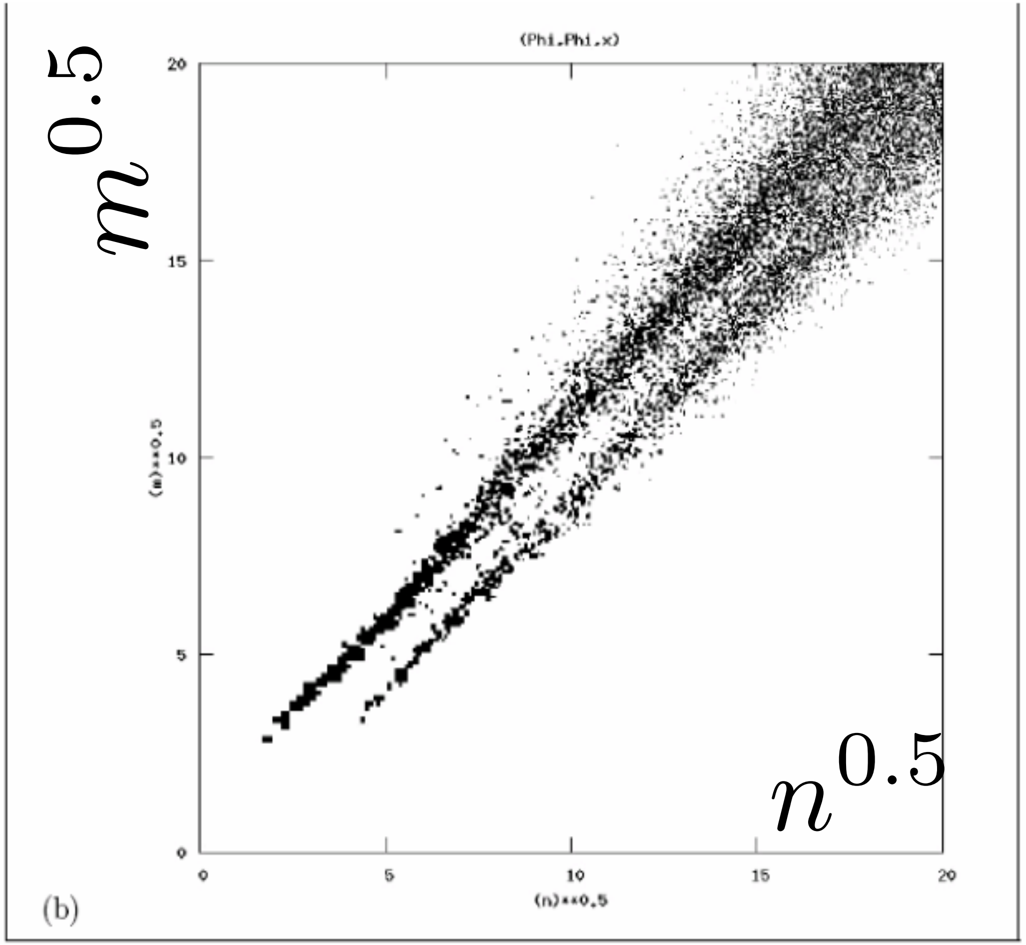

FIG. 16 – Comparison of : (a) $| < a_n \dot{a}_m > | / \lambda^{(n)}$; (b) $|(\Phi_{i,x}^{(n)} \ , \ \Phi_i^{(m)})|$. The correlations are plotted in the plane $(\sqrt{n}, \sqrt{m})$. (case **Cshort**)

$$C_{AP}(n;w) = \frac{\displaystyle\sum_{i=n-w}^{n+w} \sum_{j=(1-\alpha)i}^{(1+\alpha)i} A(i,j)P(i,j)}{\sqrt{\displaystyle\sum_{i=n-w}^{n+w} \sum_{j=(1-\alpha)i}^{(1+\alpha)i} A(i,j)^2}\sqrt{\displaystyle\sum_{i=n-w}^{n+w} \sum_{j=(1-\alpha)i}^{(1+\alpha)i} B(i,j)^2}}$$

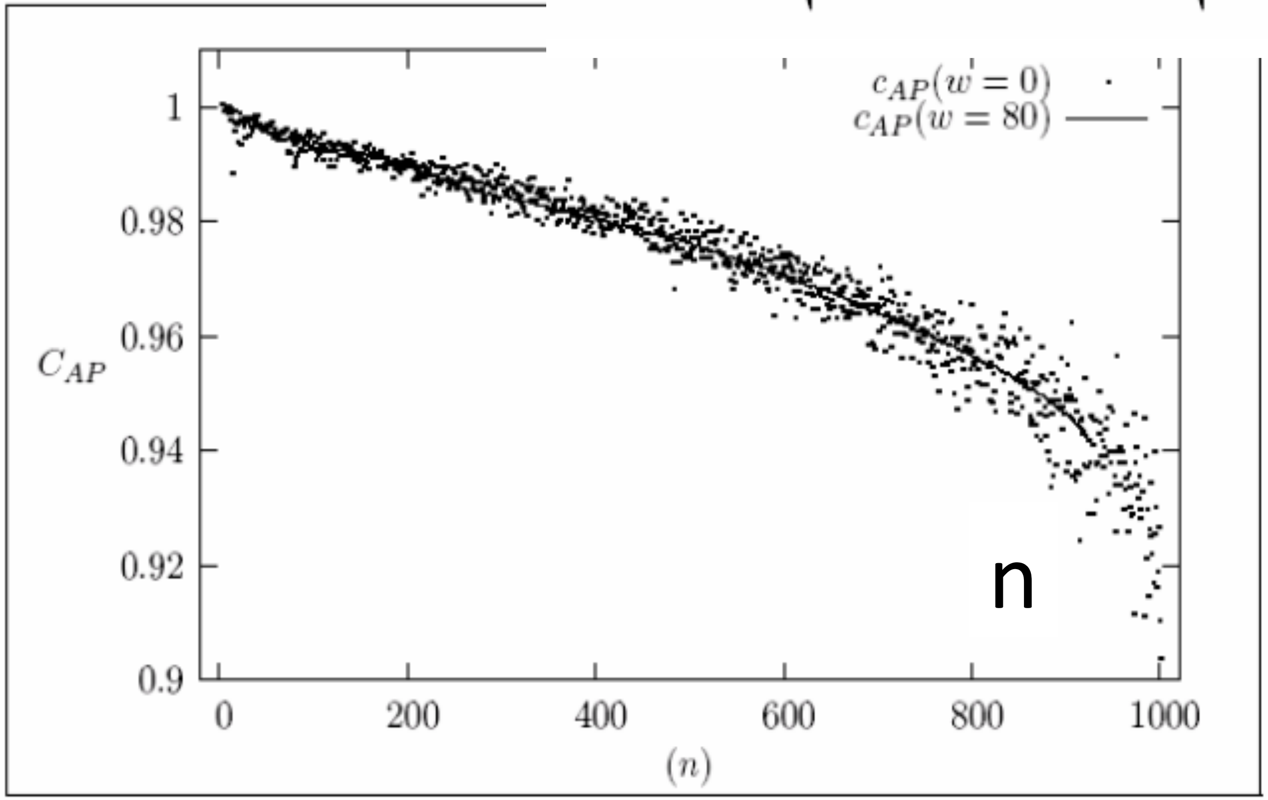

FIG. 13 – Correlation coefficient between $A(n,m)$ and $P(n,m)$ for different truncations. C_{AP} corresponds to correlation including modes 1 to (m); $C_{AP}(w=x)$ correspond to correlation where only modes $\in [m-x : m+x]$ are kept. (case **Cshort**)

$$V^{(n)} = -A(n,m)/P(n,m)$$

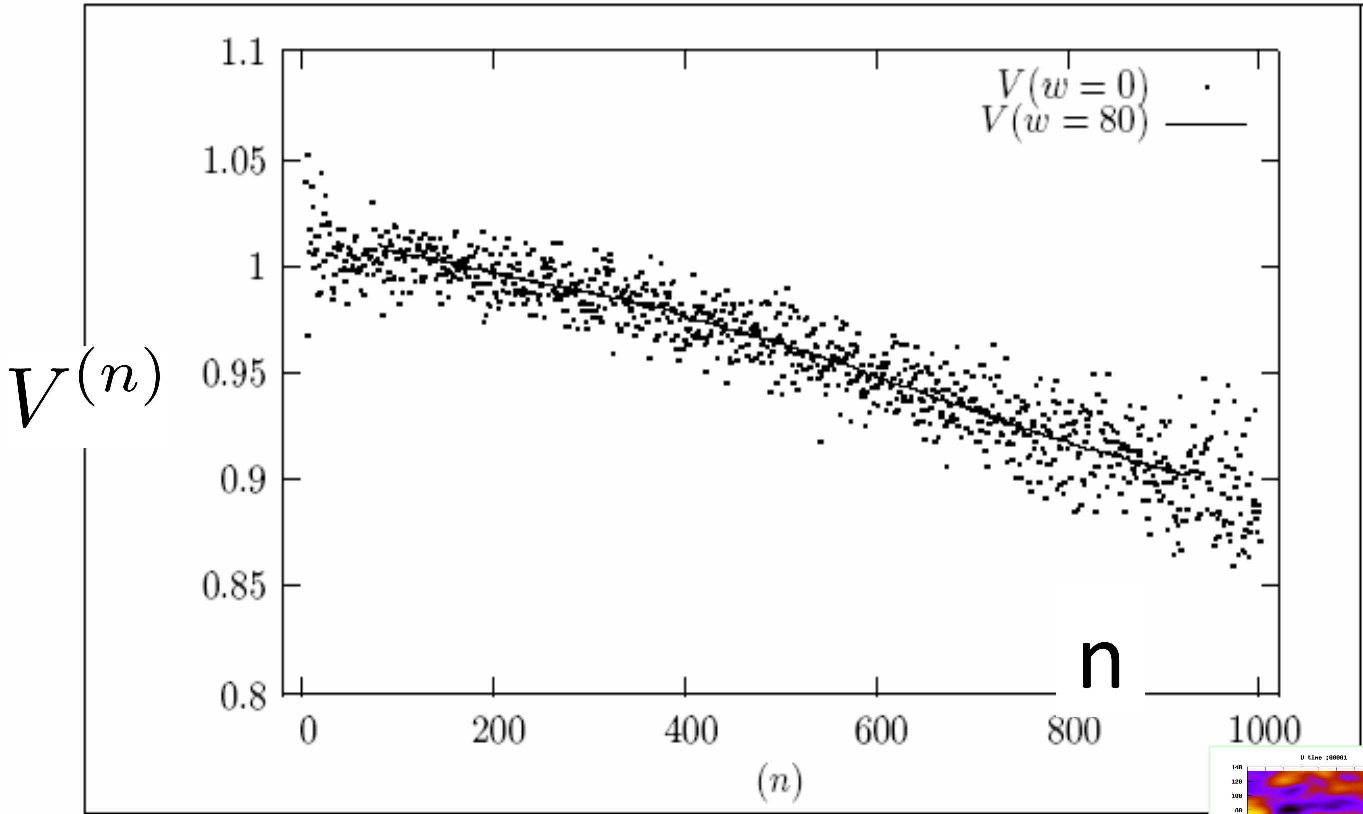

FIG. 14 – Convective velocity V obtained from a linear regression between $A(n$
See Fig. 13 for the caption.

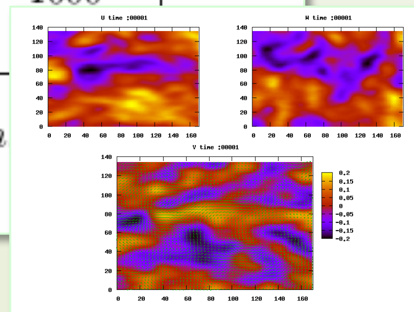

➔ A phase can be added … to the ROM

WALLTURB

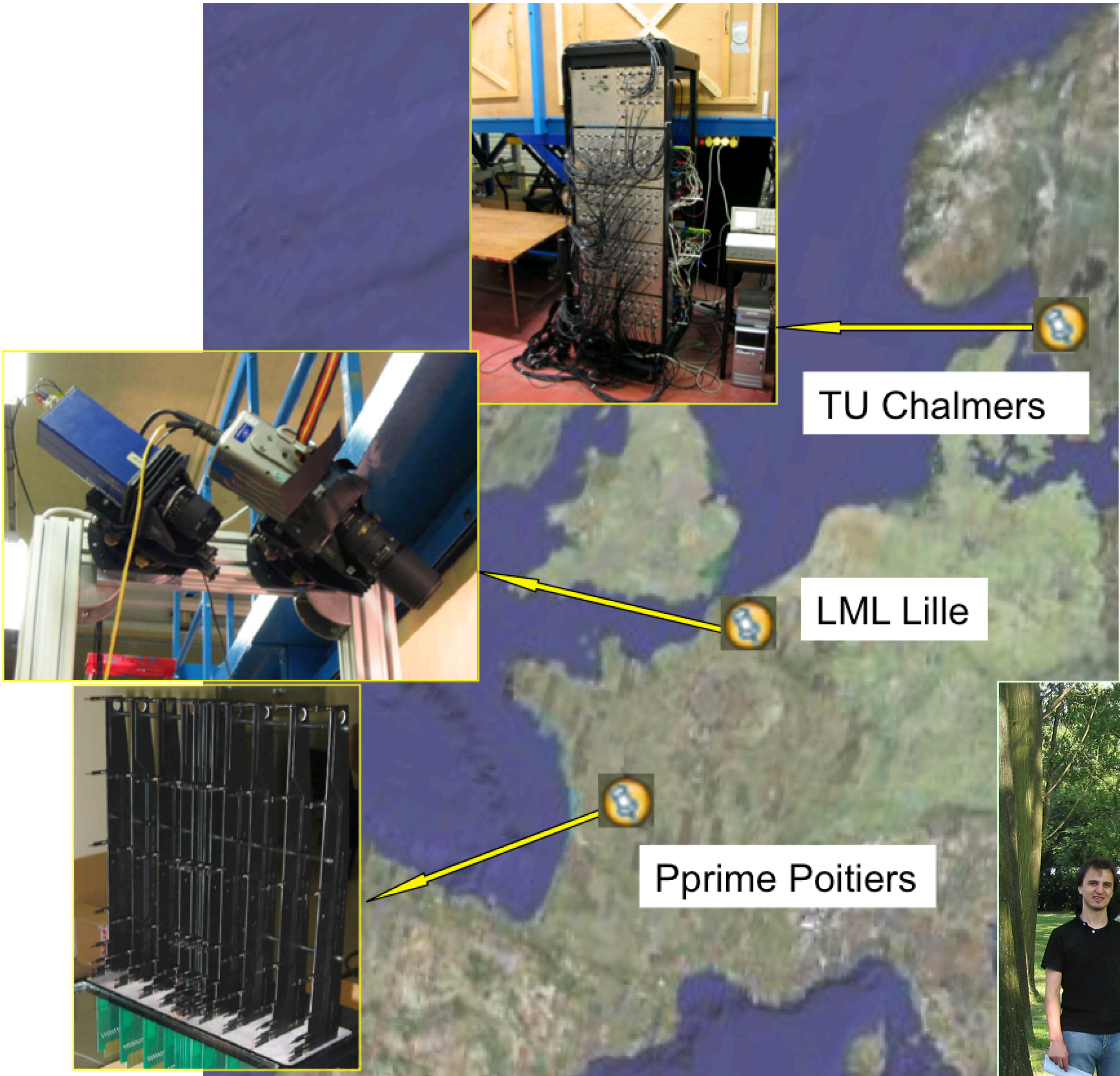

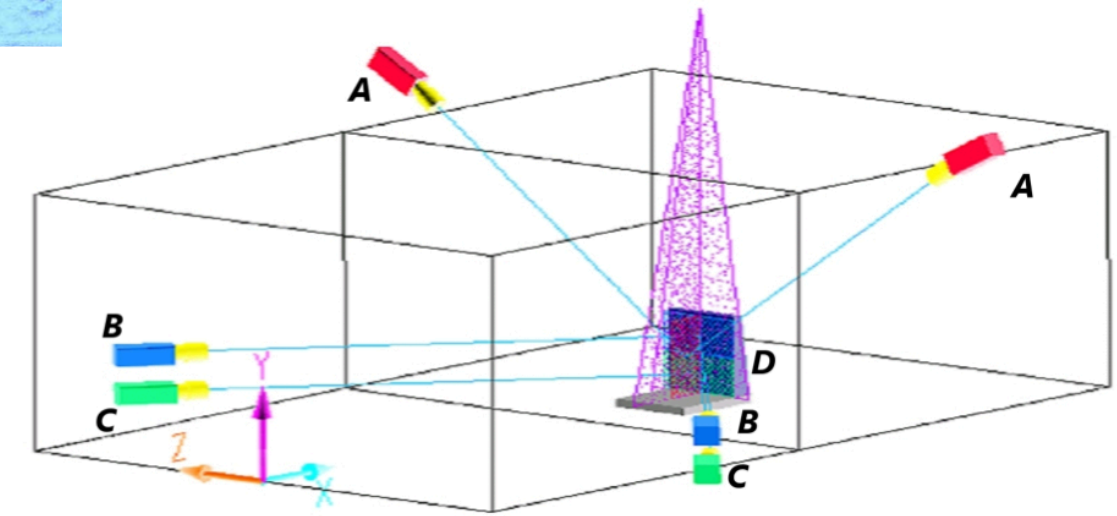

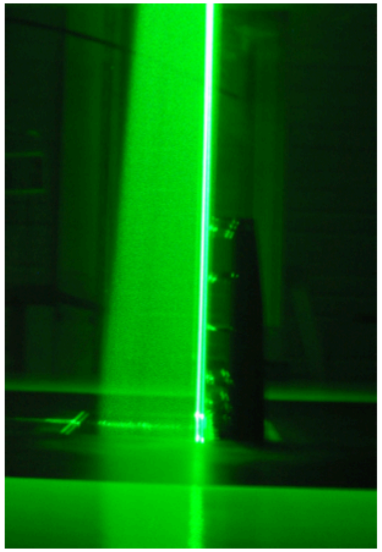

Fig. 4 Setup 1. Three stereoscopic PIV system and HWR configuration.

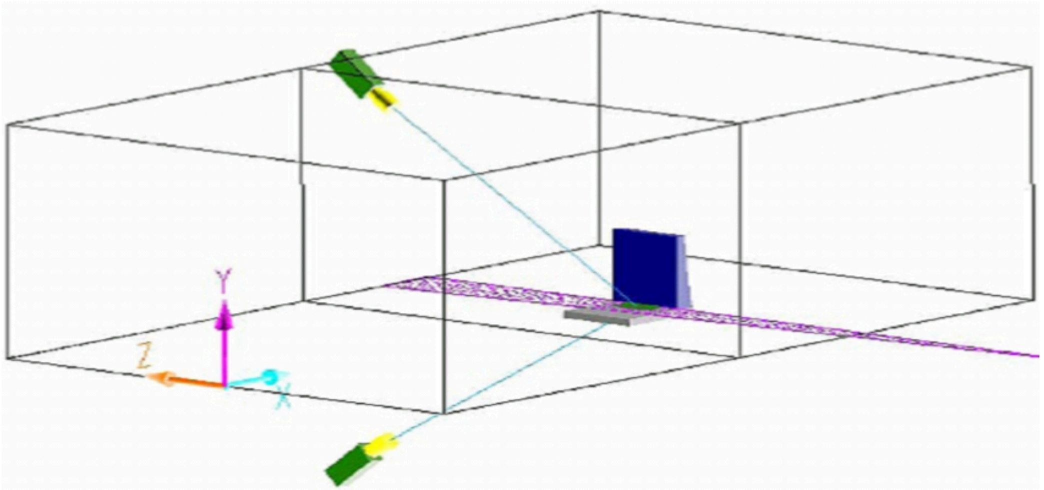

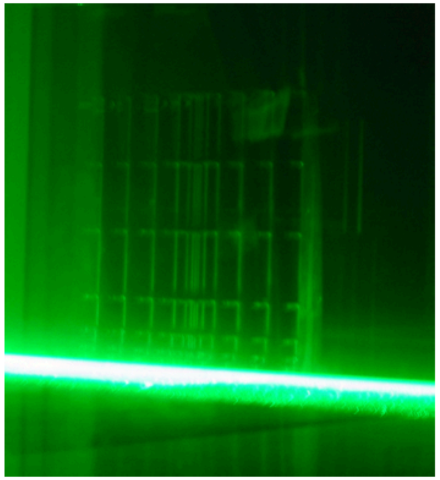

Fig. 5 Setup 2. High time rate PIV system and HWR configuration.

ZPG Turbulent Boundary Layer

Table 1 Data Base for the Zero Pressure Gradient turbulent boundary layer

U_e [m/s]	Re_θ	Configuration	No of HWR blocks (6 sec.)	No of PIV records
10	20,000	HWR + XY & YZ	600	9600
10	20,000	HWR + XZ	1100	1100× 40
10	20,000	HWR + XZ	1 block of 2.29 s	6880
10	20,000	HWR	613	0
			Total: **2314**	Total: **60480**
5	10,000	HWR + XY & YZ	600	9600
5	10,000	HWR + XZ	1100	1100× 40
5	10,000	HWR + XZ	1 block of 1.96 s	2943
5	10,000	HWR	620	0
			Total: **2321**	Total: **56543**

A data base for APG Turbulent Boundary Layer also obtained…

Instantaneous Snaphots

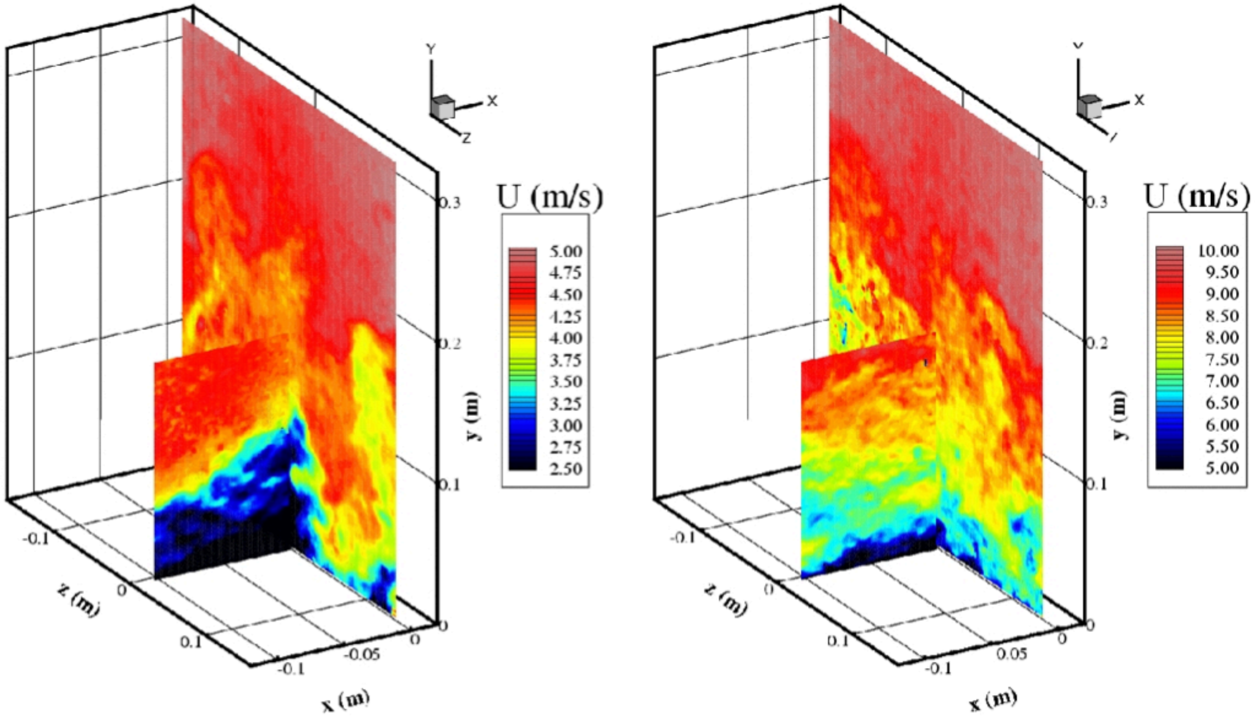

Fig. 6 Instantaneous snapshots of setup 1; U_e=5 m/s (left) ; U_e=10 m/s (right)

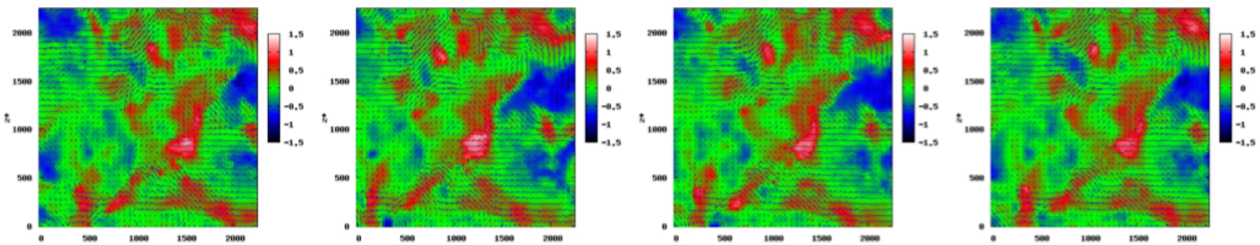

Fig. 7 Successive snapshots of setup 2

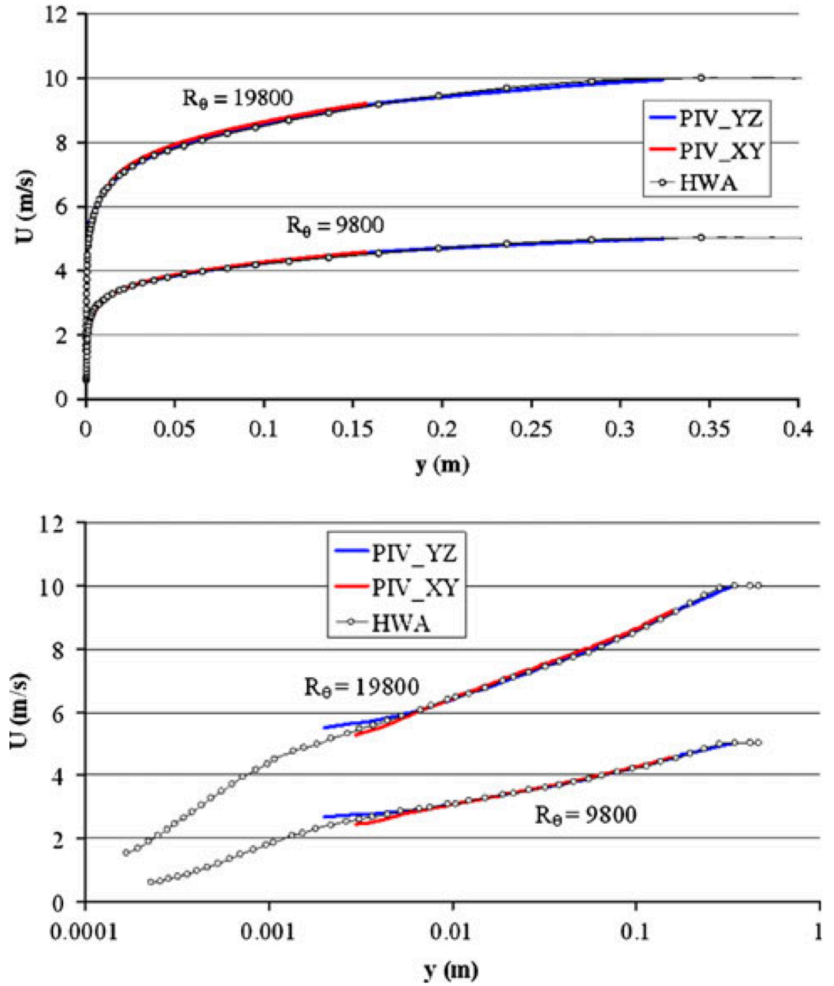

Fig. 3 Mean velocity profiles physical linear and semi-logarithmic representations

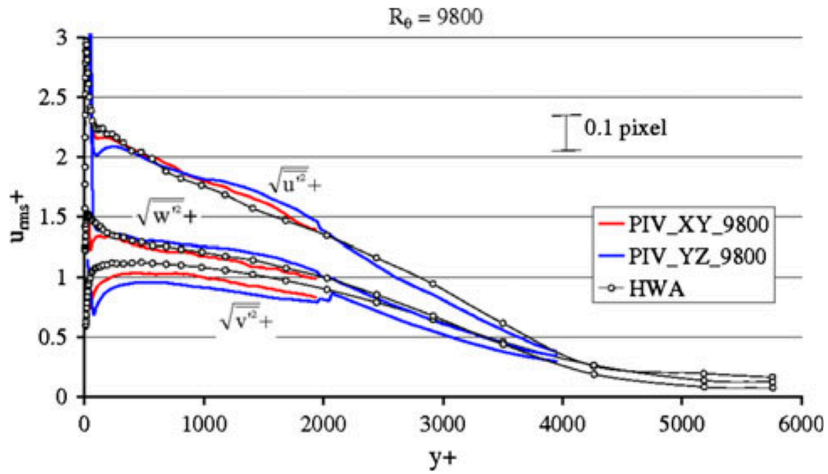

Fig. 4 Turbulence intensity profiles

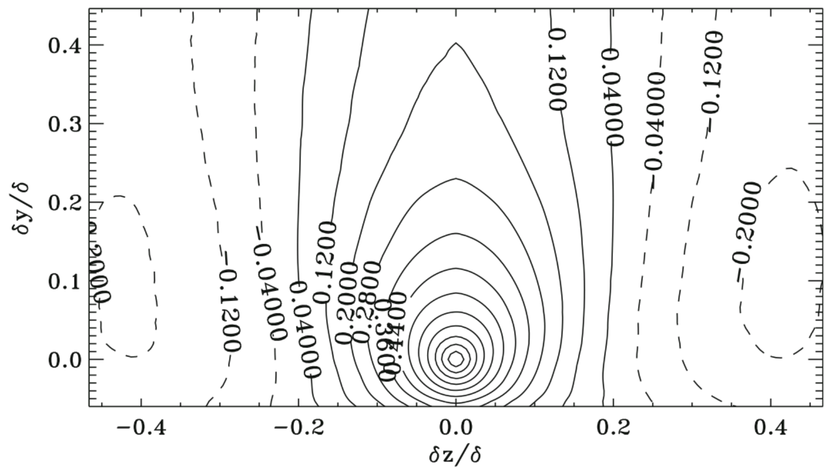

Acceleration plan parallele paroi y+=100 Rtheta7800

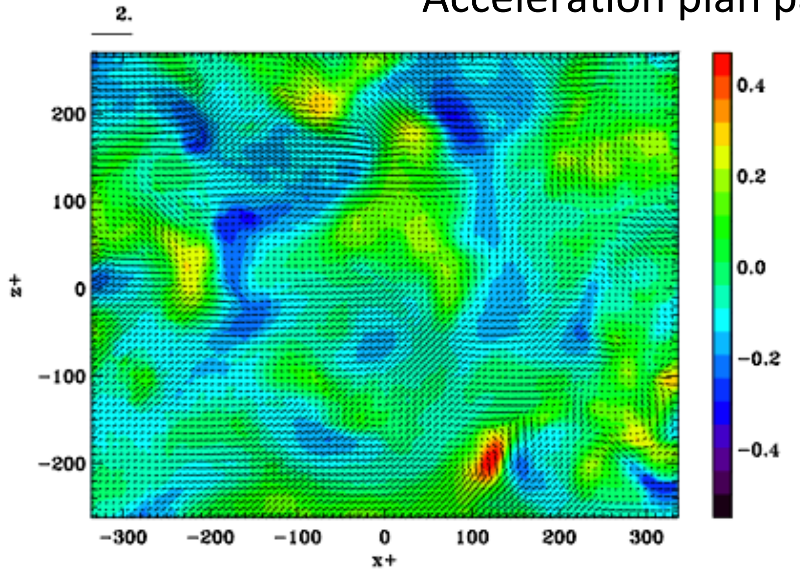

Figure 32 : Instantaneous velocity field

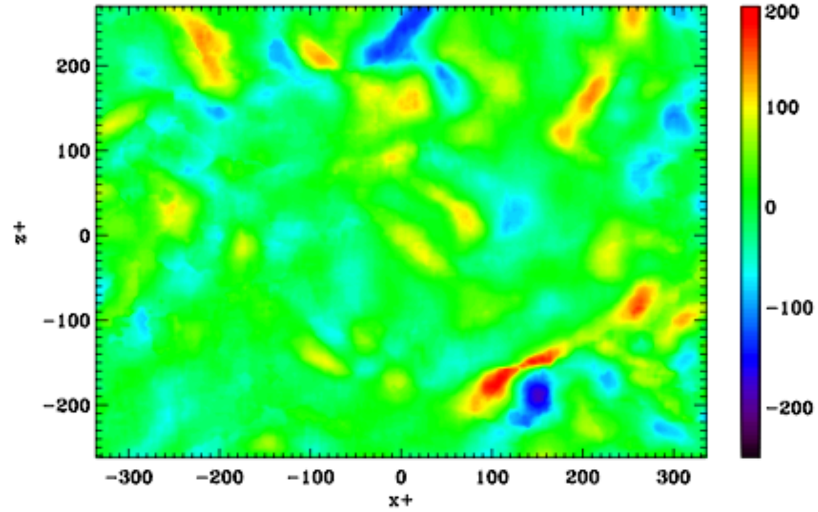

Figure 33 : Instantaneous streamwise acceleration

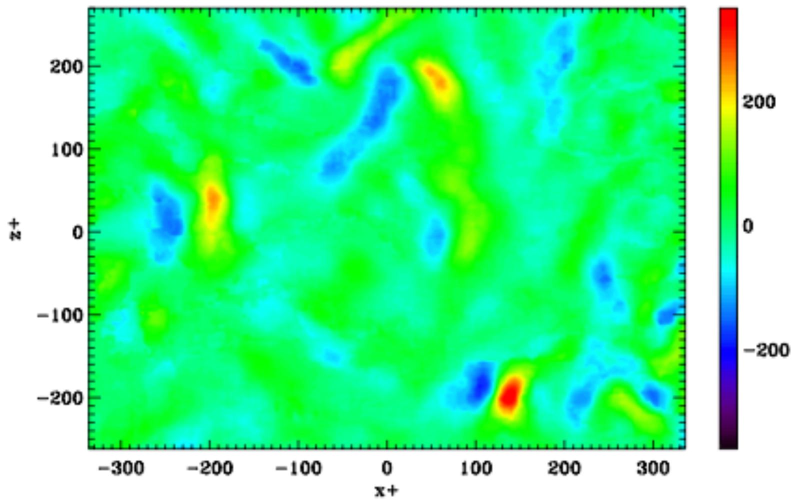

Figure 34 : Instantaneous wall normal acceleration

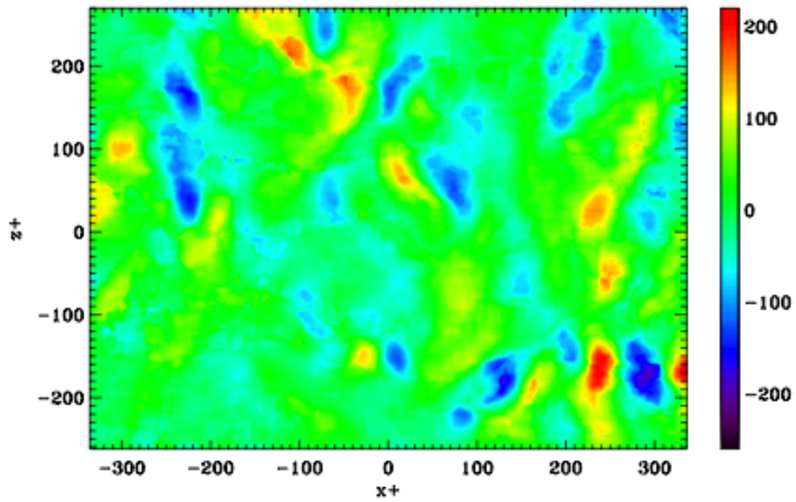

Figure 35 : Instantaneous spanwise acceleration

‘Brush‘ of 143 single hot-wires in TBL

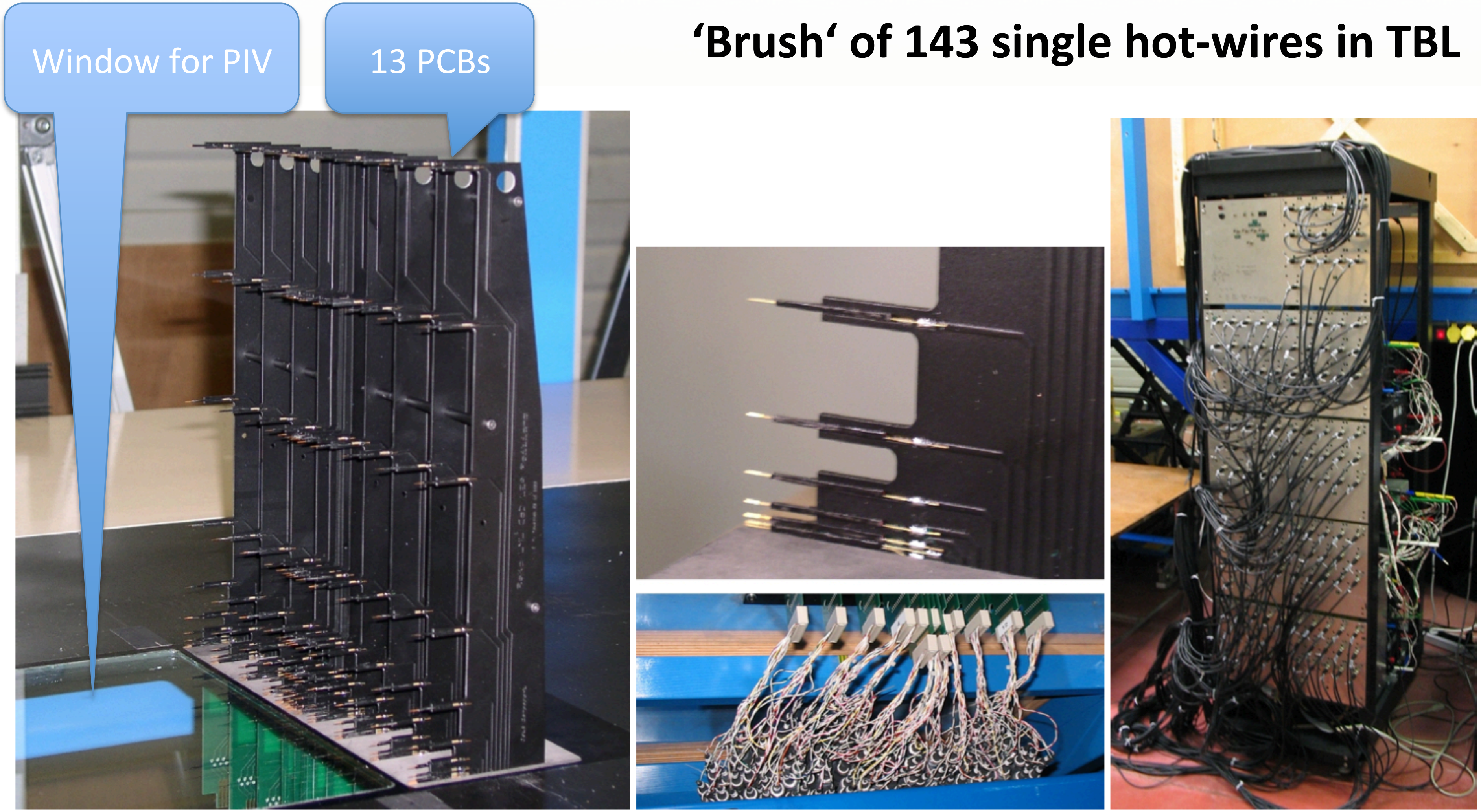

Fig. 3 The 143 hot wires rake built by LEA (left); Zoom on the closest to the wall probes of one individual comb of the rake (center - top) and view of rake connectors (center - bottom); The Chalmers constant temperature anemometers system (right).

- **Logarithmic distribution from z=± 4 mm ± 140 mm ; Smallest spanwise separation z+ = 80**
- **Logarithmic distribution from y= 0.3 to 307 mm ; First wire y+ = 6**

Hot-wire rake calibration

- Many probes to handle ➔ *in situ*
- 4 levels of external velocity : *[3, 5, 7 and 10 m/s]*
- Time consuming procedure:
    - Thermal stabilisation of the wind-tunnel
    - Convergence of statistics ➔ long duration *[50 runs of 180 000 samples of 6 s each]* ➔ *20 minutes of signal at 30kHz over 143+3 channels….*

- Use of *canonical profiles* (measured with a single hot wire)
- Use PIV measurements in cross section upstream, close to the rake to adjust calibration coefficients

- CTA deliver signals that are not linearly related to velocity

Calibration Example

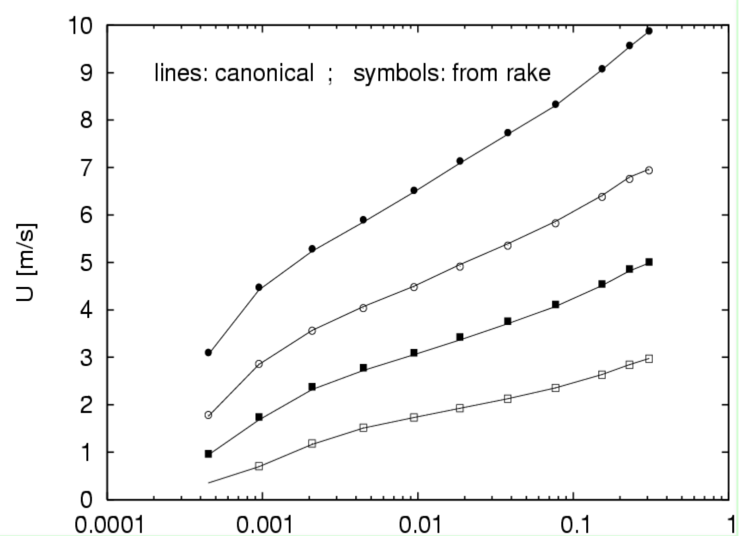

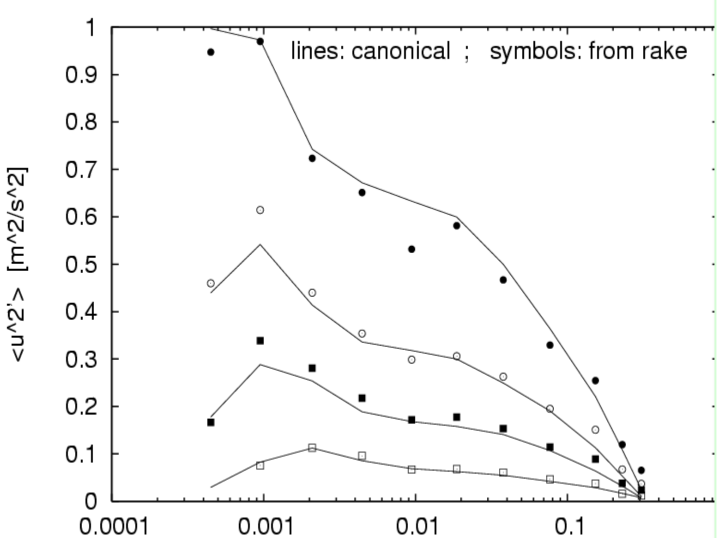

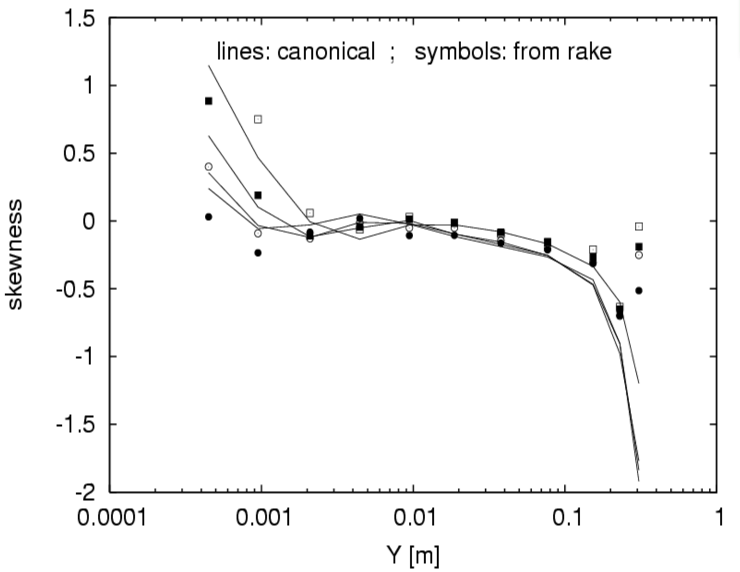

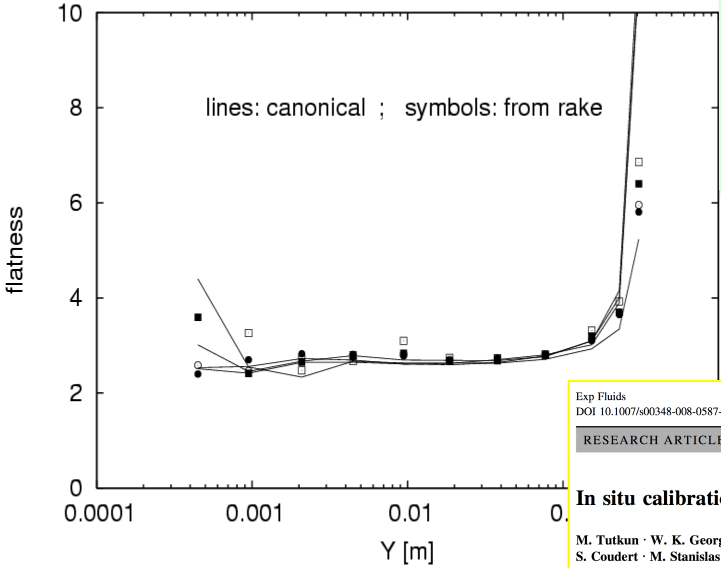

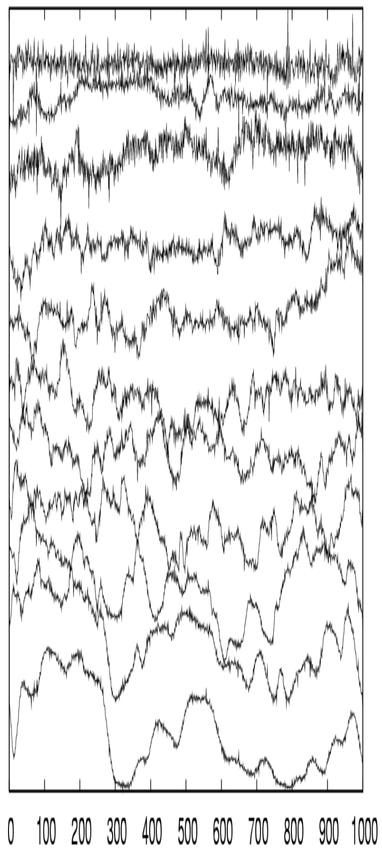

Exp Fluids
DOI 10.1007/s00348-008-0587-0

RESEARCH ARTICLE

In situ calibration of hot wire probes in turbulent flows

M. Tutkun · W. K. George · J. M. Foucaut · S. Coudert · M. Stanislas · J. Delville

Received: 30 November 2007 / Revised: 15 October 2008 / Accepted: 18 October 2008

Mean Streamwise Velocity: Setup # I

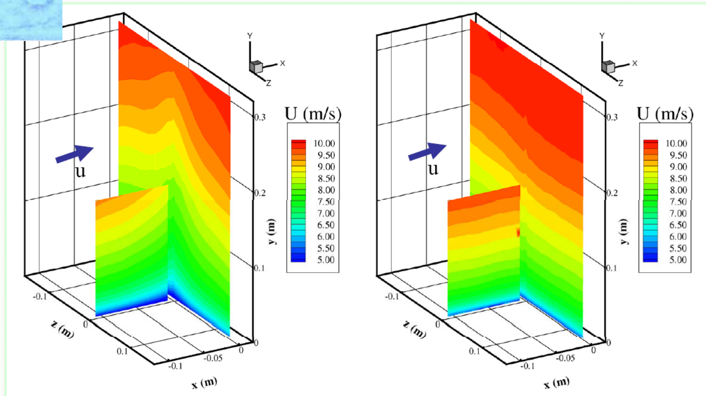

With Rake Without rake

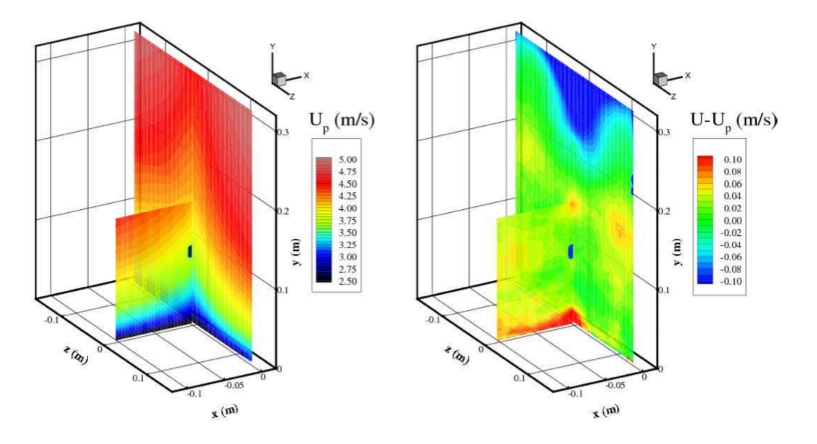

Fig. 13 Contour of the mean streamwise velocity component at 5 m/s for the potential model (a) and of the error in between model and measurement (b)

The HW-rake is 'intrusive'

blocking effect : model based on complex potential $$f(z') = \phi + i\psi = U_0.z' + \frac{m}{2\pi}\ln(z') - \frac{m}{2\pi}$$

But does not modify fluctuating parts and correlations:

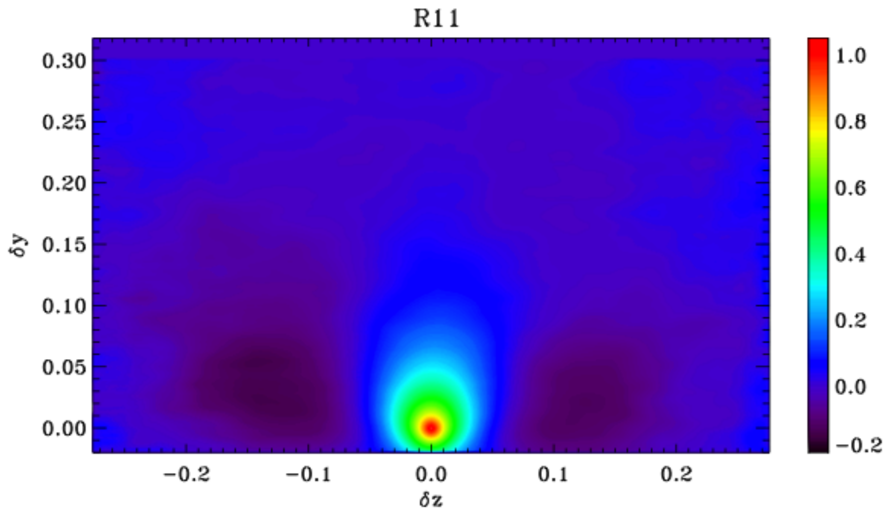

Fig. 14 Spatial correlation R_{11} in YZ plane at 10 m/s with blockage

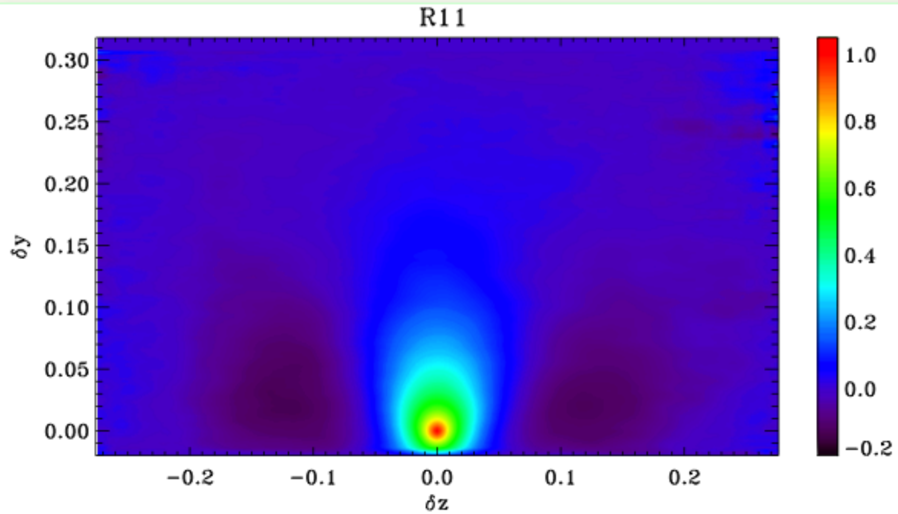

Fig. 15 Spatial correlation R_{11} in YZ plane at 10 m/s without blockage

We can reach much larger scales by using HWR

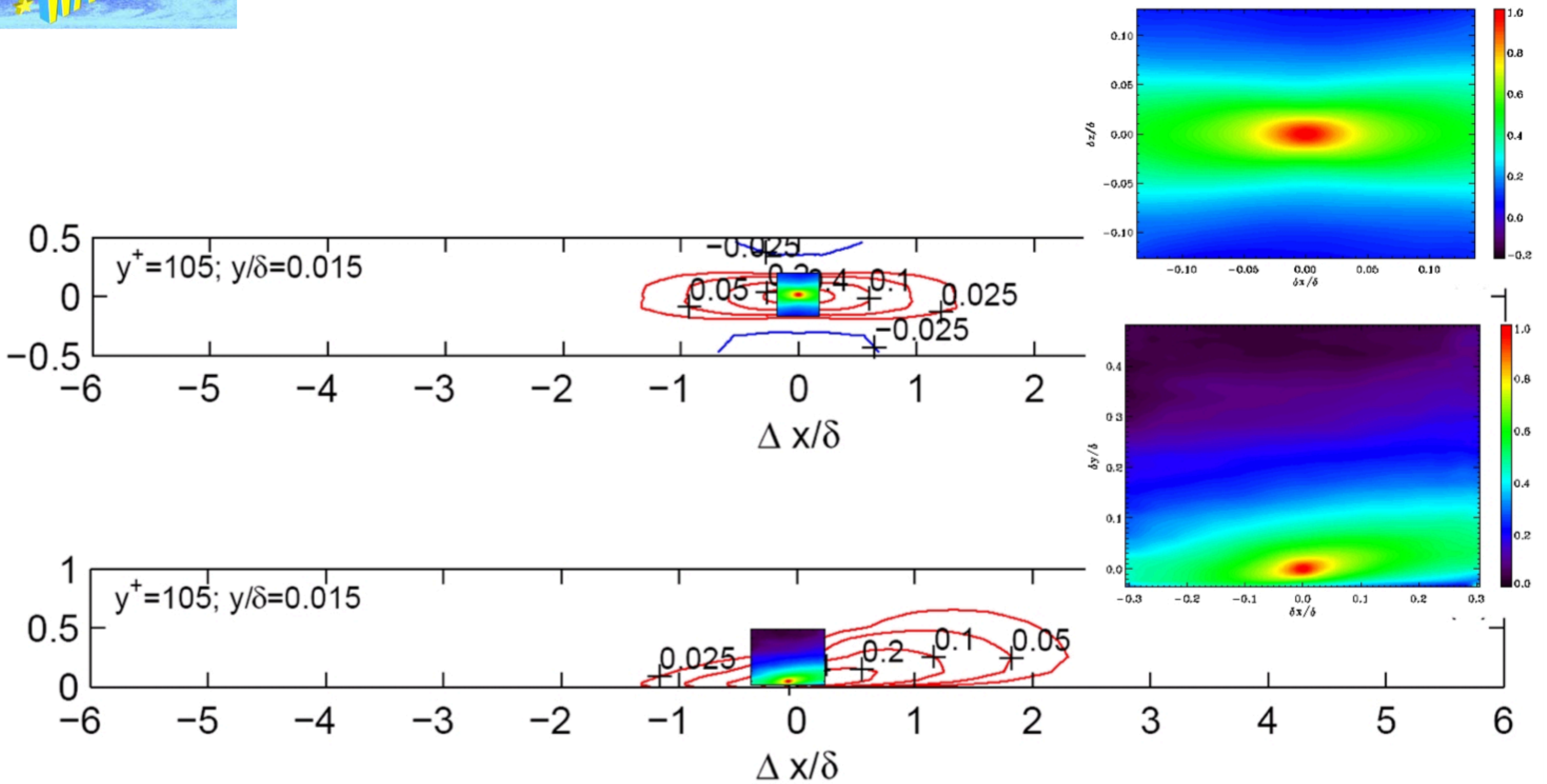

Fig. 8 Space time correlations obtained from the HWR plotted by using Taylor's hypothesis (contour lines) compared to the spatial correlations obtained from the PIV experiment (colored maps). $X-Z$ plane (top) and $X-Y$ plane (bottom).

$Re_\theta = 19000$

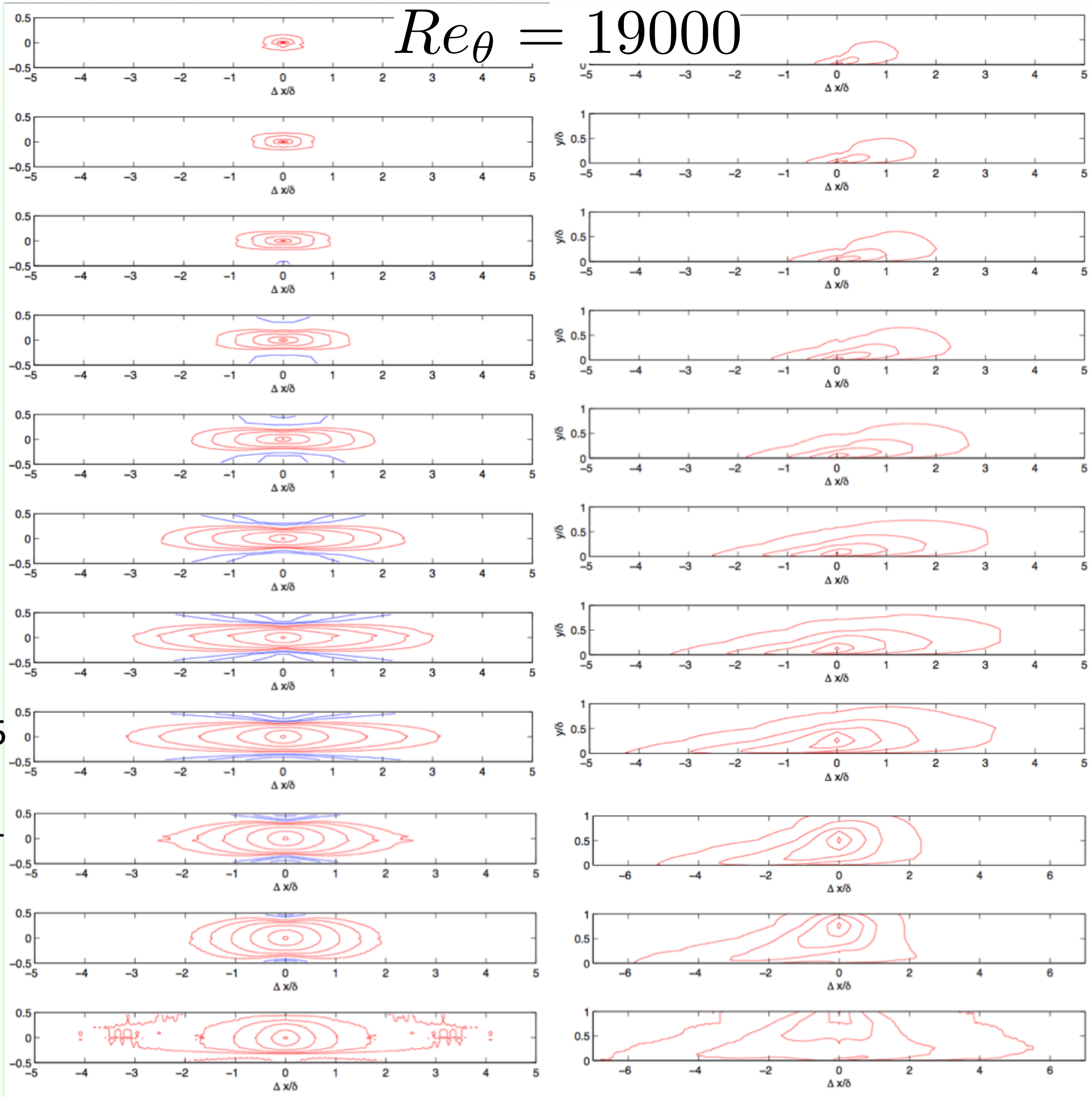

Region	y^+	y/δ
Buffer	7	0.001
	22	0.0025
	50	0.005
	100	0.01
Log law area	220	0.025
	445	0.05
	890	0.1
	1805	0.2
Outer layer		0.5
		0.75
		1

TIME-RESOLVED RECONSTRUCTION OF SUPER-STREAKS IN HIGH REYNOLDS NUMBER TURBULENT BOUNDARY LAYER OVER A FLAT PLATE

S. Roux[1], F. Kerhervé[2], J.M. Foucaut[2], M. Stanislas[2], J. Delville[3]
1 Laboratoire de Thermocinétique de Nantes UMR 6607, Université de Nantes (France)
2 Laboratoire de Mécanique de Lille, UMR CNRS 8107, EC-Lille, Univ. Lille 1 (France)
3 Institut PPRIME, CNRS UPR 3346, Université de Poitiers, ENSMA, France

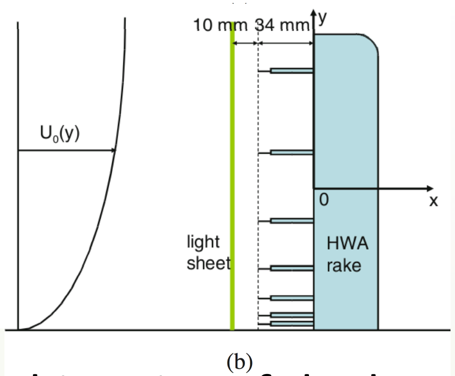

8 2013

Use L-SE to reconstruct very long time histories of the boundary layer → super-streaks

- use H-W instantaneous velocity to estimate the 2D3C velocity
- Multi time formulation: $$\hat{u}_i(\mathbf{x},t') = \sum_{k=1}^{N_h} a_{i,k}(\mathbf{x}) u^h(\mathbf{x}'_k, t' + \tau(\mathbf{x},\mathbf{x}')) \quad i = 1,2,3$$
- τ is the optimum time delay (when max of correlation)
- Linear system solved by using SVD + penalisation procedure (Tikhonov)
- Here L-SE = interpolator ..
- from 143 HW signals
- → PIV spatial resolution

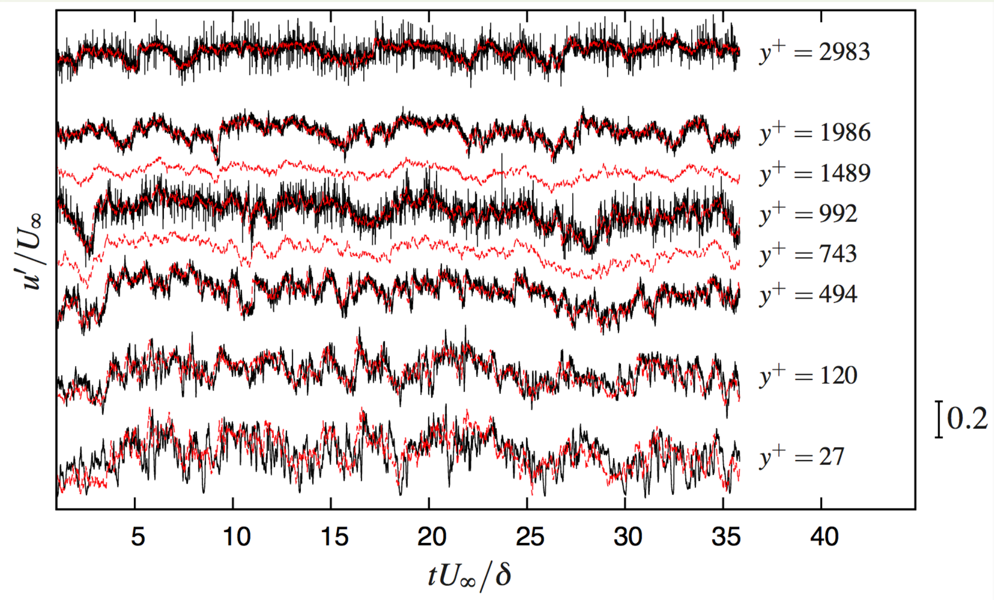

PIV → Estimated

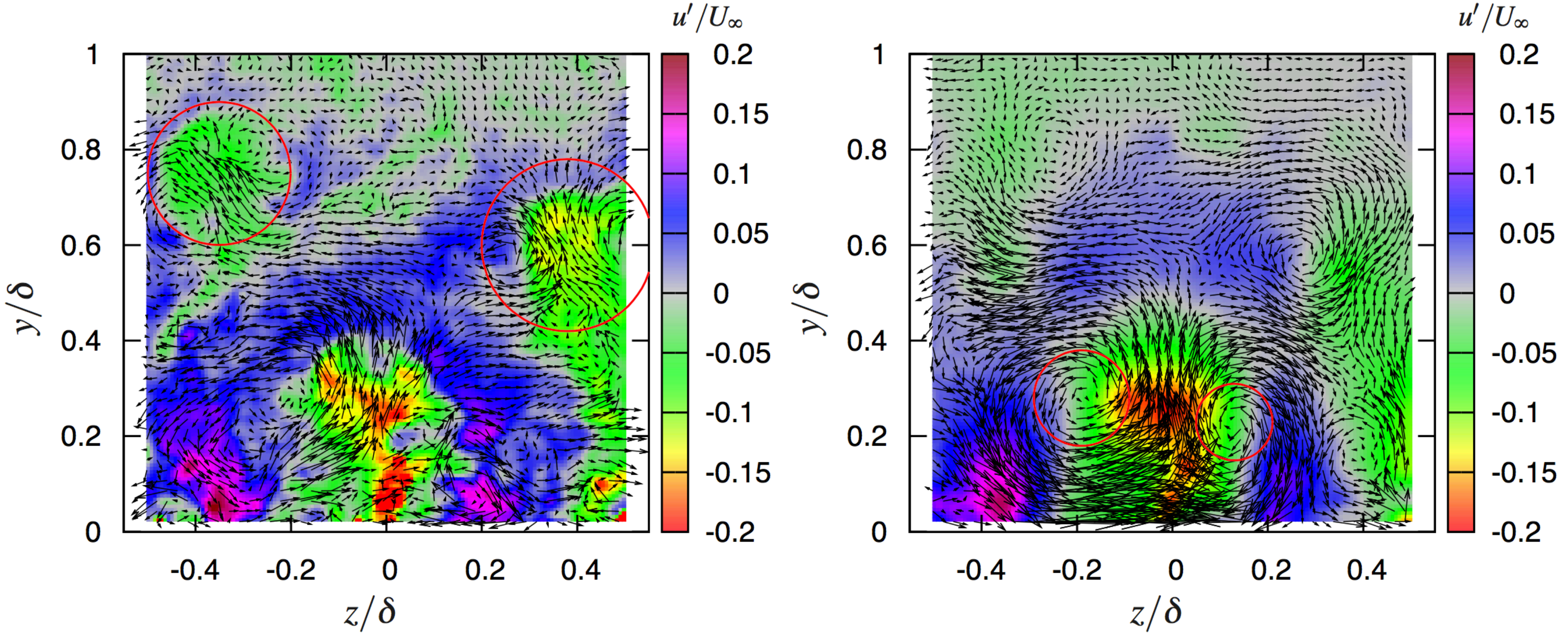

Large scale stucture filter

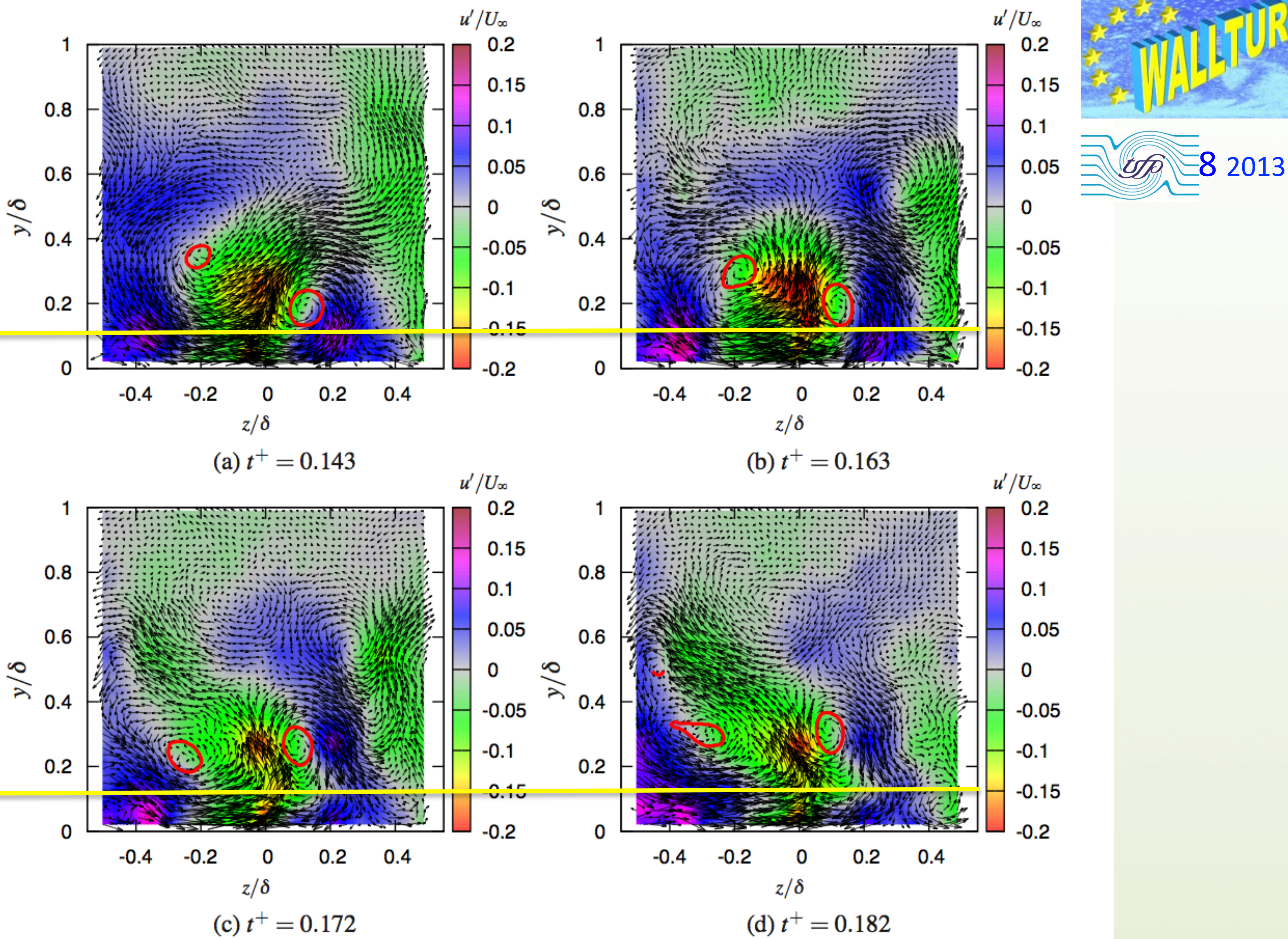

Figure 7. Conditional estimated field at different time steps. The red contours highlight center of vortical structures identified by the criteria of Graftieaux *et al*. (2001) around the low-speed streak of interest.

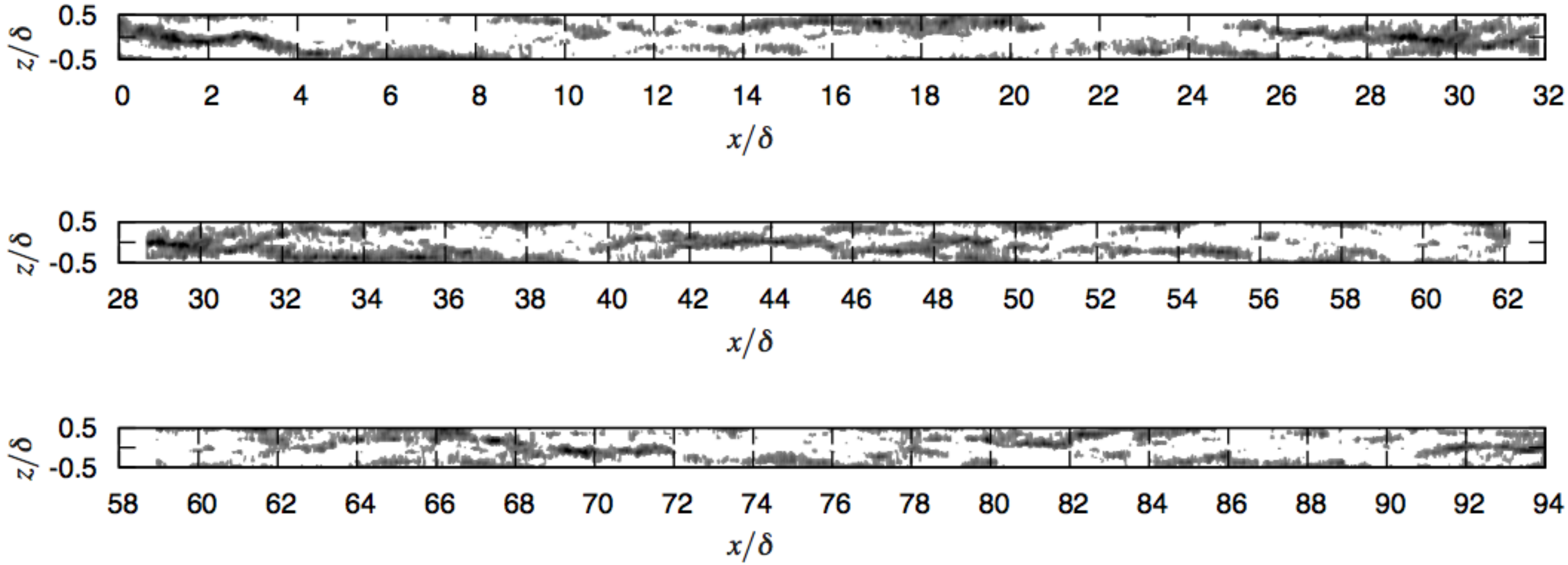

Figure 6. Reconstructed streamwise low-speed fluctuations $u'/U_\infty < -0.15$ in a plane parallel to the wall located at $y^+ = 361$ using the Taylor's hypothesis with free flow velocity.

- Wandering
- Average longitudinal Length about 10 δ

- ➔ cf Huthckins Marusic 2007

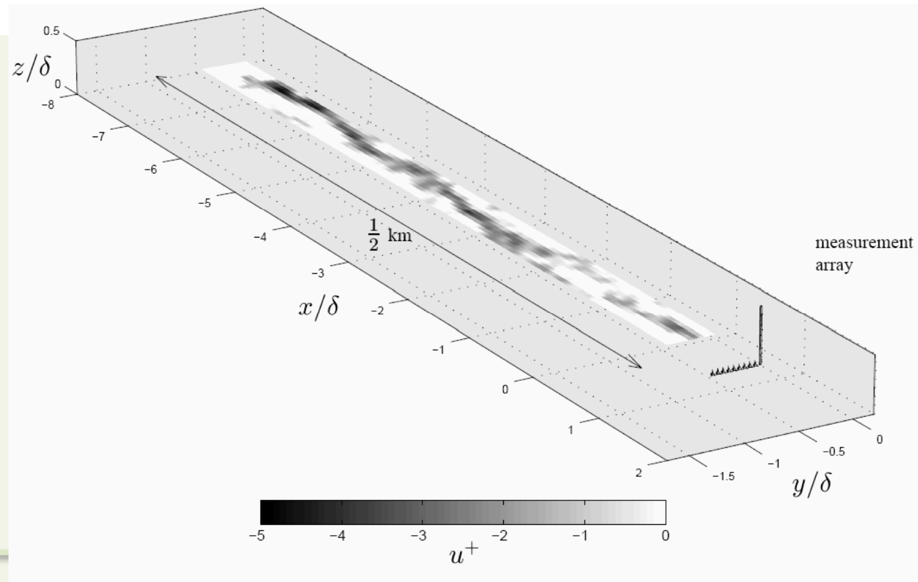

Thank you